

# Classical Limits of Scalar and Tensor Gauge Operators Based on the Overlap Dirac Matrix

Andrei Alexandru<sup>1</sup>, Ivan Horváth<sup>2</sup> and Keh-Fei Liu<sup>2</sup>

<sup>1</sup>The George Washington University, Washington, DC 20052

<sup>2</sup>University of Kentucky, Lexington, KY 40506

Jul 4 2008

## Abstract

It was recently proposed by the second author to consider lattice formulations of QCD in which complete actions, including the gauge part, are built *explicitly* from a given Dirac operator  $D$ . In a simple example of such theory, the gauge action is proportional to the trace of Ginsparg-Wilson operator  $D$  chosen to define the quark dynamics. This construction relies on the proposition that the classical limit of lattice gauge operator  $\text{tr } D(x, x)$  is proportional to  $\text{tr } F^2(x)$  (up to an additive constant). Here we show this for the case of the overlap Dirac operator using both analytical and numerical methods. We carry out the same analysis also for the tensor component of  $D$ , which is similarly related to the field-strength tensor  $F$ , and obtain results identical to our previous derivation that used different approach. The corresponding proportionality constants are computed to high precision for wide range of the negative mass parameter values, and it is verified that they are the same in finite and infinite volumes.

## 1 Introduction

To define various versions of lattice QCD (LQCD), one usually follows a standard route where the gauge part of the total continuum action is treated independently from the part involving fermions. Indeed, one normally writes down a candidate for lattice gauge action as an explicit function of link variables with appropriate symmetries, such that its continuum limit on smooth backgrounds coincides with the continuum expression. On the other hand, the basic entity in the construction of fermionic part is the lattice Dirac operator  $D$ , itself a collection of functions in gauge variables (matrix elements). In a standard treatment, one does not attempt to functionally relate gauge action to matrix elements of  $D$ .

It has recently been suggested by one of us [1, 2] that exploring lattice gauge theories with gauge and fermionic parts of the action explicitly related (*coherent LQCD*) could be beneficial for studies of QCD vacuum structure. This is particularly attractive if  $D$  is a chirally symmetric operator of Ginsparg-Wilson type.<sup>1</sup> One unusual feature of coherent

---

<sup>1</sup>It is worth emphasizing that the notion of coherent LQCD can be well-defined even if  $D$  is not chirally symmetric, assuming that a suitable function  $f(D)$  is used to define required gauge operators. For example, the choice  $f(D) = D^4$  produces coherent LQCD for arbitrary lattice Dirac operator  $D$  [1].

formulations is the possibility of incorporating explicit relations between gauge and fermionic aspects of the theory. For example, it was suggested that QCD with  $N_f$  quark flavors can be regularized via lattice formulation in which the usual gluon kinetic term is traded for additional quark flavor(s) whose mass controls the gauge coupling (symmetric logarithmic LQCD) [1, 2]. It remains to be seen if one can gain theoretical or computational advantage by introducing interrelations of this type into the lattice-regularized theory.

The validity of various coherent versions of LQCD hinges on conjectures of *locality* and proper *classical limit* for scalar and pseudoscalar gauge densities associated with operator functions  $f(D)$  used in the construction. If  $D$  is a Ginsparg–Wilson operator, which we assume from now on, then these are expected to be technically non-trivial issues due to the fact that  $D$  is necessarily a non-ultralocal operator in fermionic variables [3], and its dependence on gauge degrees of freedom is also expected to be generically non-ultralocal.

In this paper, we discuss the issue of classical limit for coherent LQCD, where the gauge action is based on  $\text{Tr } D$ . More precisely, we will focus on standard overlap operators  $D^{(\rho,r)}$  [4] constructed from Wilson–Dirac matrix (negative mass  $-\rho$ , Wilson parameter  $r$ ), and show that the classical limit of  $\text{tr } D^{(\rho,r)}(x, x)$  is proportional to  $\text{tr } F_{\mu\nu}(x)F_{\mu\nu}(x)$  up to an additive constant [1]. It should be emphasized that in formulations with  $f(D) = D$  one does not have to deal with the issue of locality. Indeed, the required locality properties follow from locality of  $D$ , which is imposed to begin with. For overlap Dirac operators the locality was studied e.g. in Refs. [5, 6], and the specific issue of locality in gauge variables was indirectly checked via reflection positivity considerations in Ref. [7].

In addition to justifying simple coherent LQCD as a valid regulator, the validity of conjectured classical limit for  $\text{tr } D^{(\rho,r)}(x, x)$  will also make possible its use as a coherent scalar partner to overlap-based pseudoscalar density (topological density) [8, 9, 10, 11]. The associated noise reduction due to non-ultralocality is expected to be useful for obtaining refined information on the fundamental vacuum structure first discovered in overlap-based topological density [12, 13], as well as for conventional uses such as studies of glueball spectrum [14]. Needless to say, for these purposes, it would in fact be desirable to have all interesting composite fields defined coherently. Important example is the field strength tensor  $F_{\mu\nu}$ , which can be constructed from tensor component of  $D^{(\rho,r)}(x, x)$  [15, 1, 16]. Direct derivation has shown that in this case the required classical limit is indeed correct [16, 17].

In principle, one could employ methods of Ref. [17] to derive the classical limit also in the scalar case considered here. However, the corresponding calculation is technically rather involved, and we thus take a different approach. In particular, the classical limit is first calculated for the class of constant gauge fields in infinite volume. This derivation is rigorous (even though technically it relies on a numerical evaluation of certain Brillouin zone integrals), and allows us to determine the corresponding proportionality constants  $c^S(\rho, r)$  in a comparably simple calculation. Next, we show that our arguments also apply for constant fields in finite volume, at least for standard periodic and antiperiodic boundary conditions. Finally, we perform a direct numerical evaluation of the classical limit on generic non-constant backgrounds and find identical results again. It is thus safe to conclude that the conjectured classical limit is indeed realized. Simultaneously with the scalar case, we apply our methods also to the tensor spinorial component and reproduce the results reported in Ref. [17], thus cross-checking both approaches. The proportionality constants  $c^S$ ,  $c^T$  and scalar subtraction constants relevant for practical applications are given.

## 2 Formulation of the Problem

Before we formulate the statements that we will be concerned with in this paper, we wish to fix our notation and specify few conventions.

(i) *Continuum Gauge Fields.* The SU(3) gauge field  $A_\mu(x)$  (traceless Hermitian  $3 \times 3$  matrices) is related to the field-strength tensor via <sup>2</sup>

$$F_{\mu\nu}(x) \equiv \partial_\mu A_\nu(x) - \partial_\nu A_\mu(x) + i[A_\mu(x), A_\nu(x)] \quad (1)$$

while the covariant derivative acts as

$$D_\mu \phi(x) = (\partial_\mu + iA_\mu(x)) \phi(x) \quad [D_\mu, D_\nu] \phi(x) = iF_{\mu\nu}(x) \phi(x) \quad (2)$$

(ii) *Classical Fields.* By classical continuum fields on  $\mathbb{R}^4$  (or on a torus) we mean gauge potentials  $A_\mu(x)$  smooth (differentiable arbitrarily many times) almost everywhere. If classical backgrounds contain singularities, the classical continuum limits are assumed to be taken at its non-singular points. While our conclusion is expected to be valid for all classical fields (due to the locality of operators involved), in what follows we will only consider classical fields that are smooth everywhere. This avoids various inessential technical complications related to transcribing singular fields on to the lattice.

(iii) *Transcription of Classical Fields to Hypercubic Lattice.* Hypercubic lattice is superimposed on  $\mathbb{R}^4$  via the correspondence  $x \equiv na$  ( $x \in \mathbb{R}^4$ ,  $n \in \mathbb{Z}^4$ ), where  $a$  is the lattice spacing. Smooth continuum field is then transcribed to the lattice field via

$$U_{n,\mu}(a) \equiv \mathcal{P} \exp \left( ia \int_0^1 ds A_\mu(an + (1-s)a\hat{\mu}) \right) \quad (3)$$

where  $\mathcal{P}$  is the path ordering symbol and  $\hat{\mu}$  is a unit vector in direction  $\mu$ .

(iv) *Overlap Operators.* Standard overlap Dirac operators are defined by [4]

$$D^{(\rho,r)} = \rho [1 + \mathcal{X}(\mathcal{X}^\dagger \mathcal{X})^{-\frac{1}{2}}] \quad \mathcal{X} = D_W - \rho \quad \rho \in (0, 2r) \quad r > 0 \quad (4)$$

where  $D_W \equiv 4r \mathbb{I} - \frac{1}{2}K$  is the massless Wilson-Dirac operator and  $K$ , the Wilson's hopping matrix with Wilson parameter  $r$ , is given by

$$K_{n,m} = \sum_\mu (r - \gamma_\mu) U_{n,\mu} \delta_{n+\mu,m} + (r + \gamma_\mu) U_{n-\mu,\mu}^\dagger \delta_{n-\mu,m} \quad (5)$$

For calculations in this paper, it is convenient to work with the rescaled matrix  $\mathcal{X}$  namely

$$\mathcal{X} \longrightarrow X \equiv 2\kappa \mathcal{X} = \mathbb{I} - \kappa K \quad \kappa \equiv \frac{1}{8r - 2\rho} \quad (6)$$

The form of the overlap operator (4) in terms of  $\mathcal{X}$  is identical to that in terms of  $X$ .

---

<sup>2</sup>Note that this differs from conventions of Ref. [1], where anti-Hermitian gauge potentials were used instead. The equations used here can be obtained from equations of Ref. [1] via substitutions  $A_\mu(x) \rightarrow iA_\mu(x)$ ,  $F_{\mu\nu}(x) \rightarrow iF_{\mu\nu}(x)$ . The values of constants  $c^S$ ,  $c^T$  are the same in both conventions.

(v) *Classical Limit Conjecture.* Our main goal in this paper is to support the Conjecture C3 of Ref. [1] for the specific case of standard overlap Dirac operators. In the infinite volume, one can state this as follows.<sup>3</sup>

**Conjecture 1.** *Let  $A_\mu(x)$  be arbitrary smooth  $SU(3)$  gauge potentials on  $\mathbb{R}^4$ . If  $U(a) \equiv \{U_{n,\mu}(a)\}$  is the transcription of this field to the hypercubic lattice with classical lattice spacing  $a$ , and  $\mathbb{I} \equiv \{U_{n,\mu} \rightarrow \mathbb{I}_c\}$  is the free gauge configuration then*

$$\text{tr}_{sc} \left( D_{0,0}(U(a)) - D_{0,0}(\mathbb{I}) \right) = c^S a^4 \text{tr}_c F_{\mu\nu}(0) F_{\mu\nu}(0) + \mathcal{O}(a^6) \quad (7)$$

where  $D \equiv D^{(\rho,r)}$  is the overlap Dirac operator and  $F_{\mu\nu}(x)$  is the field-strength tensor associated with  $A_\mu(x)$ . The constant  $c^S \equiv c^S(\rho, r)$  is non-zero and independent of  $A_\mu(x)$  at fixed  $\rho$  and  $r$ .

We will also discuss classical limits for tensor components of  $D^{(\rho,r)}$ . The corresponding statement is obtained from the above by replacing Eq. (7) with [1, 17]

$$\text{tr}_s \sigma_{\mu\nu} D_{0,0}(U(a)) = c^T a^2 F_{\mu\nu}(0) + \mathcal{O}(a^4) \quad (8)$$

where  $\sigma_{\mu\nu} \equiv \frac{1}{2i}[\gamma_\mu, \gamma_\nu]$ .<sup>4</sup>

We emphasize that the above statements (with identical proportionality constants  $c^S(\rho, r)$ ,  $c^T(\rho, r)$ ) are also expected to be true in a finite volume. We will verify this here for the practically relevant case of a torus. In what follows, we will frequently skip explicitly denoting dependences of operators/constants on parameters  $\rho$  and  $r$ , but they are implicitly understood.

### 3 Constant Fields in Infinite Volume

In this section we establish that the leading term of Eq. (7) is indeed correct for the class of constant gauge fields  $A_\mu(x) \equiv A_\mu$ . This is the simplest class of classical fields leading to non-zero field-strength tensor (for non-Abelian gauge fields), while the resulting simplifications make the calculation reasonably manageable.

For constant classical backgrounds the transcribed lattice field at lattice spacing  $a$  has the simple form<sup>5</sup>

$$U_{n,\mu}(a) = \exp(iaA_\mu) \quad (9)$$

and the overlap Dirac matrix is translation invariant  $D_{n,m} = D_{n-m,0}$ . The calculation of classical limit simplifies in the Fourier space, where the operator is diagonal in space-time

---

<sup>3</sup>The subscripts “s”, “c” in expressions that follow refer to “spin” and “color” respectively. Thus, for example,  $\mathbb{I}_c$  denotes the identity matrix in color space ( $3 \times 3$  matrix) and  $\text{tr}_{sc}$  denotes the trace in both spin and color.

<sup>4</sup> We use Hermitian  $\gamma$ -matrices  $\gamma_\mu^\dagger = \gamma_\mu$  throughout this paper.

<sup>5</sup>It is worth mentioning at this point that one can use perturbation theory techniques to obtain expansions needed [10, 18, 19, 20]. Here we proceed without reference to weak coupling perturbation theory, as done in [11, 17].

indices. For arbitrary translation invariant operator  $O_{n,m}$  we define the diagonal Fourier image  $O(k)$  via

$$O(k) \equiv \sum_n e^{-i(n-m)k} O_{n,m} \quad O_{n,m} = \frac{1}{(2\pi)^4} \int d^4k e^{i(n-m)k} O(k) \quad (10)$$

where the integration over momentum variables runs through the Brillouin zone. The definition of  $O(k)$  requires the convergence of the above infinite sum, for which it is sufficient that  $O$  is local. For arbitrary constant gauge field  $A_\mu$  the overlap Dirac operator  $D$  in transcribed lattice background  $U_\mu(a)$  is guaranteed to be local [5] at sufficiently small classical lattice spacing  $a$ , and thus its Fourier transform is well defined.

To evaluate  $D(k)$ , we start from the expression for  $D$  in terms of matrix  $X$  (see Eq. (6))

$$\frac{1}{\rho} D = \mathbb{I} + X \frac{1}{\sqrt{X^\dagger X}} \quad (11)$$

The Fourier transform  $X(k)$  of  $X$  can be found straightforwardly and is given by

$$X(k) = \mathbb{I}_{sc} - 2\kappa r \sum_\mu \cos(aA_\mu + k_\mu) + i 2\kappa \sum_\mu \gamma_\mu \sin(aA_\mu + k_\mu) \quad (12)$$

Moreover, the Hermitian matrix  $B \equiv X^\dagger X$  is strictly positive-definite for sufficiently small  $a$  in arbitrary constant background [5].<sup>6</sup> Consequently, the Fourier image of  $B^{-1/2}$  is simply given by  $(X^\dagger(k)X(k))^{-1/2}$ , and thus

$$\frac{1}{\rho} D(k) = \mathbb{I}_{sc} + X(k) \frac{1}{\sqrt{X^\dagger(k)X(k)}} \quad (13)$$

### 3.1 Expansion in Lattice Spacing

For the purposes of Conjecture 1, we are interested in the Taylor expansion (in  $a$ ) of

$$\frac{1}{\rho} D_{0,0} = \frac{1}{\rho} \frac{1}{(2\pi)^4} \int d^4k D(k) = \mathbb{I}_{sc} + \frac{1}{(2\pi)^4} \int d^4k X(k) \frac{1}{\sqrt{X^\dagger(k)X(k)}} \quad (14)$$

which can be obtained term by term from the Taylor expansion of  $X(k)B^{-1/2}(k)$  due to its analyticity in both  $k$  and  $a$  for sufficiently small  $a$ .

To fix the notation that we will use for various operators, we generically write

$$O(k, a) = \sum_{n=0}^{\infty} O_n(k) a^n \equiv O_0(k) + \delta O(k, a) \quad (15)$$

where the dependence of  $O(k)$  on  $a$  will usually not be shown explicitly. The leading terms for  $X(k)$  and  $B(k)$  are given by<sup>7</sup>

$$X_0(k) = 1 - 2\kappa r \sum_\mu \cos k_\mu + i 2\kappa \sum_\mu \gamma_\mu \sin k_\mu \quad (16)$$

---

<sup>6</sup>The gap in the spectrum of  $B$  tends to zero when excluded boundary values  $\rho = 0$  and  $\rho = 2r$  are approached.

<sup>7</sup>Note that in the formulas that follow we denote  $\mathbb{I}_{sc}$  simply as “1” with spin-color structure understood.

and

$$B_0(k) = \left(1 - 2\kappa r \sum_{\mu} \cos k_{\mu}\right)^2 + 4\kappa^2 \sum_{\mu} \sin^2 k_{\mu} \quad (17)$$

There are two points to note here. (i)  $B_0(k)$  is proportional to identity and is positive-definite for all  $k$ , except when  $\kappa r = 1/8, 1/4$  which corresponds to excluded boundary values of the  $\rho$ -parameter 0,  $2r$ . This means that  $B_0(k)$  can be commuted and inverted freely in the expressions that follow. (ii) The matrices  $\delta X(k)$  and  $\delta B(k)$  have norms that can be made arbitrarily small by lowering the lattice spacing sufficiently, and can thus serve as “perturbations” in matrix expansions around  $X_0(k)$  and  $B_0(k)$ .

The expansion of  $X(k)B^{-1/2}(k)$  in lattice spacing, needed in (14), can now proceed via expanding  $X(k)$  and  $B^{-1/2}(k)$  separately and then combining the results. In case of  $X(k)$ , the expansion is obtained directly from (12), while for  $B^{-1/2}(k)$  we use

$$B^{-\frac{1}{2}} = (B_0 + \delta B)^{-\frac{1}{2}} = B_0^{-\frac{1}{2}} (1 + \tilde{\delta} B)^{-\frac{1}{2}} \quad \tilde{\delta} B \equiv B_0^{-1} \delta B \quad (18)$$

Properties (i) and (ii) guarantee that  $\tilde{\delta} B$  is a valid perturbation for the expansion of the inverse square root, yielding

$$B^{-\frac{1}{2}} = B_0^{-\frac{1}{2}} \left[ 1 - \frac{1}{2} \tilde{\delta} B + \frac{3}{8} (\tilde{\delta} B)^2 - \frac{5}{16} (\tilde{\delta} B)^3 + \frac{35}{128} (\tilde{\delta} B)^4 \right] + \mathcal{O}((\tilde{\delta} B)^5) \quad (19)$$

Note that we have to keep all the terms up to the 4-th order since we are eventually interested in  $\mathcal{O}(a^4)$  contribution and  $\tilde{\delta} B$  is  $\mathcal{O}(a)$ . Indeed, the explicit formula for  $B(k)$  in terms of its Clifford decomposition is given by

$$B(k) = \mathbb{I}_s \times \mathcal{S}(k) + \gamma_{\mu} \times \mathcal{V}_{\mu}(k) + \sigma_{\mu\nu} \times \mathcal{T}_{\mu\nu}(k) \quad (20)$$

where

$$\mathcal{S}(k) = \left(1 - 2\kappa r \sum_{\mu} \cos(aA_{\mu} + k_{\mu})\right)^2 + 4\kappa^2 \sum_{\mu} \sin^2(aA_{\mu} + k_{\mu}) \quad (21)$$

$$\mathcal{V}_{\mu}(k) = i4\kappa^2 \sum_{\nu} \left[ \sin(aA_{\mu} + k_{\mu}), \cos(aA_{\nu} + k_{\nu}) \right] \quad (22)$$

$$\mathcal{T}_{\mu\nu}(k) = i2\kappa^2 \left[ \sin(aA_{\mu} + k_{\mu}), \sin(aA_{\nu} + k_{\nu}) \right] \quad (23)$$

and  $[,]$  denotes the commutator. From this one can inspect directly that while  $\mathcal{V}_{\mu}$  and  $\mathcal{T}_{\mu\nu}$  are  $\mathcal{O}(a^2)$ , the scalar part contains both the constant and the linear term, and thus  $\tilde{\delta} B$  is indeed  $\mathcal{O}(a)$ .

The equations of this subsection together with Eq. (12) define the procedure of evaluating various classical limits completely. The calculation is straightforward, but turns out to be technically still quite involved if one wants to obtain a complete expansion of  $D(k)$  (and thus of  $D_{0,0}$ ) all the way up to order  $a^4$ .

### 3.2 Sample Computation – First Order

To see the characteristic nature of the computations involved, let us now expand  $D(k)$  up to order  $a$ . For this purpose, we will need expansions of  $X(k)$  and  $B(k)$  up to  $\mathcal{O}(a)$ . We find

$$X(k) = X_0(k) + a \sum_{\mu} A_{\mu} \underbrace{2\kappa (r \sin k_{\mu} + i\gamma_{\mu} \cos k_{\mu})}_{g_{\mu}(k)} + \mathcal{O}(a^2) \quad (24)$$

and

$$B(k) = B_0(k) + a \sum_{\mu} A_{\mu} \underbrace{\left[ 4\kappa r (1 - 2\kappa r \sum_{\nu} \cos k_{\nu}) \sin k_{\mu} + 8\kappa^2 \sin k_{\mu} \cos k_{\mu} \right]}_{f_{\mu}(k)} + \mathcal{O}(a^2) \quad (25)$$

Note that  $f_{\mu}(k)$  comes entirely from  $\mathcal{S}(k)$ . Using the expansion (19) up to  $\mathcal{O}(\tilde{\delta}B)$  we then obtain  $D(k) = D_0(k) + aD_1(k) + \mathcal{O}(a^2)$  where

$$\frac{1}{\rho} D_0(k) = 1 + B_0(k)^{-1/2} X_0(k) \quad (26)$$

and

$$\frac{1}{\rho} D_1(k) = \sum_{\mu} A_{\mu} \underbrace{B_0(k)^{-3/2} \left[ g_{\mu}(k) B_0(k) - \frac{1}{2} f_{\mu}(k) X_0(k) \right]}_{h_{\mu}(k)} \quad (27)$$

The leading term  $D_0(k)$  is the Fourier transform of the free overlap operator as expected.

Let us now focus on the first-order term which will determine (after inverse Fourier transform) the first-order term of  $D_{0,0}$ . Using transformation properties, one can argue that this first-order term should in fact vanish. Indeed,  $D_{0,0}$  is a gauge covariant operator and this covariance has to be preserved order by order in the Taylor expansion. Thus, the coefficient of the linear term is expected to be a dimension one (continuum) gauge covariant operator (spin-color function of the gauge field), but such operator does not exist. On the other hand, the result (27) shows that  $D_1(k)$  is not identically zero. This does not imply any contradiction as long as the associated inverse Fourier expression vanishes. One can see that this is indeed the case by evaluating  $h_{\mu}(k)$  of Eq. (27) explicitly, yielding

$$h_{\mu}(k) = h_{\mu}^A(k) + i\gamma_{\mu} h_{\mu}^S(k) \quad (28)$$

where  $h_{\mu}^A(k)$  is antisymmetric with respect to  $k_{\mu} \rightarrow -k_{\mu}$ , while  $h_{\mu}^S(k)$  is symmetric, fully diagonal and can be written as a derivative, namely <sup>8</sup>

$$h_{\mu}^S(k) = 2\kappa \frac{\partial}{\partial k_{\mu}} \sin k_{\mu} B_0^{-\frac{1}{2}}(k) \quad (29)$$

Consequently,  $\int d^4k D_1(k) = 0$  and we have

$$D_{0,0}(U(a)) = D_{0,0}(\mathbb{I}) + \mathcal{O}(a^2) \quad (30)$$

While relatively simple, this calculation fully illustrates the issues encountered also at higher orders, where the number of terms to deal with grows rather quickly.

---

<sup>8</sup>We thank the referee for pointing this out to us.

### 3.3 Tensor Component and the Second Order

The tensor part of  $D_{0,0}$  first appears at second order in classical lattice spacing. Using the technique described above we straightforwardly arrive (see also Appendix A) at the expression in Fourier space, namely

$$\frac{1}{\rho} D_2(k) = \sum_{\mu\nu} \left[ \frac{1}{4} \frac{2r}{(4r - \rho)^3} \frac{t_{\mu\nu}(k)}{B_0^{3/2}(k)} \right] \sigma_{\mu\nu} \times F_{\mu\nu} + \dots \quad (31)$$

where  $F_{\mu\nu} = i[A_\mu, A_\nu]$ ,  $\sigma_{\mu\nu} = \frac{1}{2i}[\gamma_\mu, \gamma_\nu]$ , and “...” represents terms that are either odd in  $k_\mu$  or are partial derivatives of analytic functions with respect to  $k_\mu$ , thus not contributing upon transition back from Fourier space. The expression in the bracket is a real-valued function of the momentum and it should be pointed out that from now on we use the symbol  $B_0(k)$  to interchangeably denote a color-spin matrix proportional to identity, as well as its diagonal matrix element. The function  $t_{\mu\nu}(k)$  is given by

$$t_{\mu\nu}(k) = \sin^2 k_\mu \cos k_\nu + \sin^2 k_\nu \cos k_\mu - \left( 4 - \frac{\rho}{r} - \sum_\alpha \cos k_\alpha \right) \cos k_\mu \cos k_\nu \quad (32)$$

The constant  $c^T = c^T(\rho, r)$  of Eq. (8) is then specified by

$$c^T(\rho, r) = \frac{2r\rho}{(4r - \rho)^3} \frac{1}{(2\pi)^4} \int d^4k \frac{t_{\mu\nu}(k)}{B_0^{3/2}(k)} \quad (33)$$

and doesn't depend on  $\mu, \nu$  due to hypercubic symmetries. One can easily check that this result is identical to the one we obtained previously in Ref. [17].

The parameter dependence of  $c^T$  is more transparent if one introduces a rescaled mass parameter

$$\hat{\rho} \equiv \frac{\rho}{r} \quad \hat{\rho} \in (0, 2) \quad (34)$$

and the rescaled  $B_0(k)$ , namely

$$z(k) \equiv \frac{1}{(2\kappa)^2} B_0(k) = (4r - \rho)^2 B_0(k) \quad (35)$$

With that we finally have

$$c^T(\hat{\rho}, r) = 2\hat{\rho} r^2 \int \frac{d^4k}{(2\pi)^4} \frac{t_{\mu\nu}(k)}{z^{3/2}(k)} \quad (36)$$

where

$$z(k) = \sum_\mu \sin^2(k_\mu) + r^2 \left( 4 - \hat{\rho} - \sum_\mu \cos k_\mu \right)^2 \quad (37)$$

depends on both  $\hat{\rho}$  and  $r$ , while

$$t_{\mu\nu}(k) = \sin^2 k_\mu \cos k_\nu + \sin^2 k_\nu \cos k_\mu - \left( 4 - \hat{\rho} - \sum_\alpha \cos k_\alpha \right) \cos k_\mu \cos k_\nu \quad (38)$$



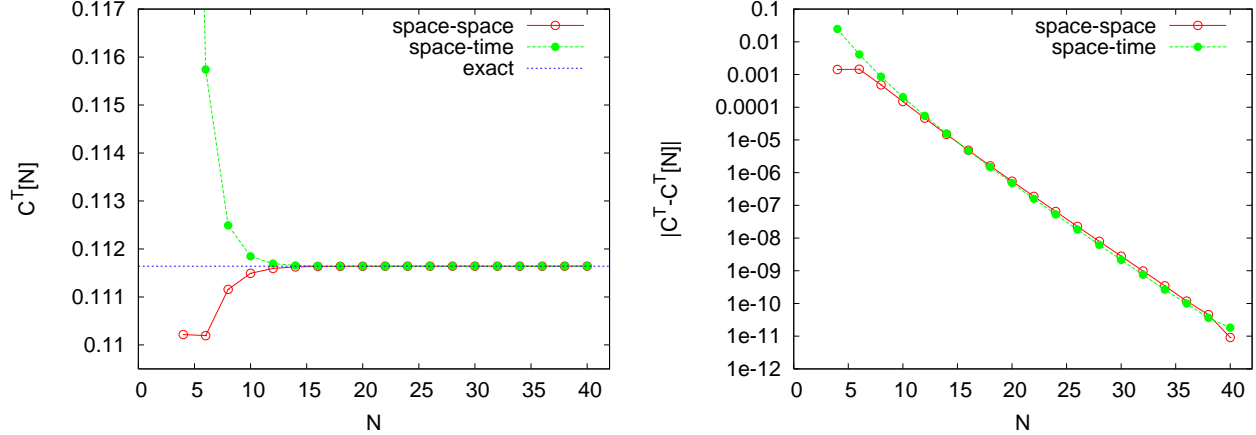


Figure 1: Riemann sums for proportionality constant  $c^T$  of the tensor term. These results were computed at  $r = 1$  and  $\kappa = 0.19$  ( $\rho = 26/19$ ).

only depends on  $\hat{\rho}$ .

For explicit evaluation of  $c^T$  we study the convergence of Riemann sums associated with the corresponding Brillouin zone integral. More precisely, we partition the integration domain  $[0, 2\pi]^4$  into  $N^4$  cubes of volume  $(2\pi/N)^4 \equiv (\delta k)^4$  and define the corresponding Riemann sum  $c^T[N]$  via

$$\frac{1}{2\hat{\rho}r^2} c^T[N] \equiv \frac{1}{(2\pi)^4} \sum_k (\delta k)^4 \frac{t_{\mu\nu}(k)}{z^{3/2}(k)} = \frac{1}{N^4} \sum_k \frac{t_{\mu\nu}(k)}{z^{3/2}(k)} \quad (39)$$

where the discrete momenta associated with elementary cubes have components

$$k_\mu = \begin{cases} (\delta k) l_\mu & \text{for } \mu = 1, 2, 3 \\ (\delta k) (l_\mu + 1/2) & \text{for } \mu = 4 \end{cases} \quad l_\mu = 0, 1, \dots, N-1 \quad (40)$$

Note that this choice of discrete momenta exactly corresponds to the situation on the latticized torus of size  $N$  with mixed periodic (spatial) and antiperiodic (time) boundary conditions, which is frequently a preferred setup in finite volume.<sup>9</sup> Due to the asymmetric choice of the discretization, the value of  $c^T[N]$  at finite  $N$  will depend on whether the pair  $\mu, \nu$  chosen for evaluation is of space-space or space-time kind, but the difference has to vanish in the  $N \rightarrow \infty$  limit. In Fig. 1 we show the dependence of  $c^T[N]$  on  $N$  for both cases, showing that they converge exponentially in  $N$  to the common non-zero limit. The value labeled as “exact” includes only digits determined to be stabilized under increasing  $N$  in the calculation.

### 3.4 Scalar Component and the Fourth Order

Our main goal in this paper is the evaluation of classical limit for the scalar spinorial component of  $D_{0,0}$ , and its complete trace in particular. Since the expectation is that the leading term (up to a constant to be subtracted) will appear at the 4-th order, one has to carry out

<sup>9</sup>The rationale for this is that it will allow us to argue that, for constant fields, our results on infinite lattice can be mapped exactly to this specific finite-volume case.

expansions described in Secs. 3.1, 3.2 up to that order. Algebraic manipulations involved in this are rather extensive and we have used *Mathematica* for required symbolic manipulations. The result can be written in the form

$$\text{tr}_{sc} D_{0,0}(U(a)) = \text{tr}_{sc} D_{0,0}(\mathbb{I}) + a^4 I_4 + \mathcal{O}(a^6) \quad (41)$$

The odd powers are absent in the scalar spinorial component (do not contribute upon taking the spinorial trace of  $D_{0,0}$ ). The quartic term is given by

$$I_4 = \sum_{\mu} i_{4,\mu} \text{tr}_c A_{\mu}^4 + \sum_{\mu < \nu} \alpha_{\mu\nu} \text{tr}_c A_{\mu} A_{\mu} A_{\nu} A_{\nu} + \sum_{\mu < \nu} \beta_{\mu\nu} \text{tr}_c A_{\mu} A_{\nu} A_{\mu} A_{\nu} \quad (42)$$

To describe the results of calculation for constants  $i_{4,\mu}$ ,  $\alpha_{\mu\nu}$ ,  $\beta_{\mu\nu}$  we now have to introduce few conventions. All the coefficients to compute will be defined by functions in the momentum space of the form

$$\hat{F}(k; j, \hat{c}) = \frac{1}{B_0(k)^j} \sum_n \hat{c}(n) \cos(k_1)^{n_1} \cos(k_2)^{n_2} \cos(k_3)^{n_3} \cos(k_4)^{n_4} \quad (43)$$

where  $n \equiv (n_1, n_2, n_3, n_4)$  is a four-component vector of non-negative integers,  $j$  is a single half-integer and  $\hat{c}(n)$  is real-valued. Each function of interest is thus specified by  $j$  and the finite list of non-zero coefficients  $\hat{c}(n)$ .

To reduce the amount of information needed for evaluation of the coefficients, we will use the fact that, by means of the inverse Fourier transform, it is only the mean value of  $\hat{F}$  that is relevant. More precisely, we are interested only in

$$F(j, \hat{c}) \equiv \int \frac{d^4 k}{(2\pi)^4} \hat{F}(k; j, \hat{c}) = \sum_n \hat{c}(n) I(j, n) \quad (44)$$

where we introduced the notation  $I(j, n)$  for integrals of the form

$$I(j, n) \equiv \int \frac{d^4 k}{(2\pi)^4} \frac{\cos(k_1)^{n_1} \cos(k_2)^{n_2} \cos(k_3)^{n_3} \cos(k_4)^{n_4}}{B_0(k)^j} \quad (45)$$

Since  $I(j, n)$  is completely symmetric with respect to indices  $n_{\mu}$ , we can restrict the sum over  $n$  in (44) only to  $n$  such that  $n_1 \geq n_2 \geq n_3 \geq n_4$ , and redefine the coefficients  $\hat{c}(n) \rightarrow c(n)$  accordingly. We then have

$$F(j, c) \equiv \sum_{n_1 \geq n_2 \geq n_3 \geq n_4} c(n) I(j, n) \quad (46)$$

and we specify our results by listing  $j$  and  $c(n)$  for each case in question.

The last piece of convention we need to specify concerns the choice of discretization for performing Riemann sums in the actual evaluation of momentum integrals. While final results have to be independent of that choice, our discussion of classical limits in the finite volume (see Sec. 4) can be mapped directly on the discussion here if Riemann sums are defined in a particular manner. Moreover, consistency over different discretizations represents

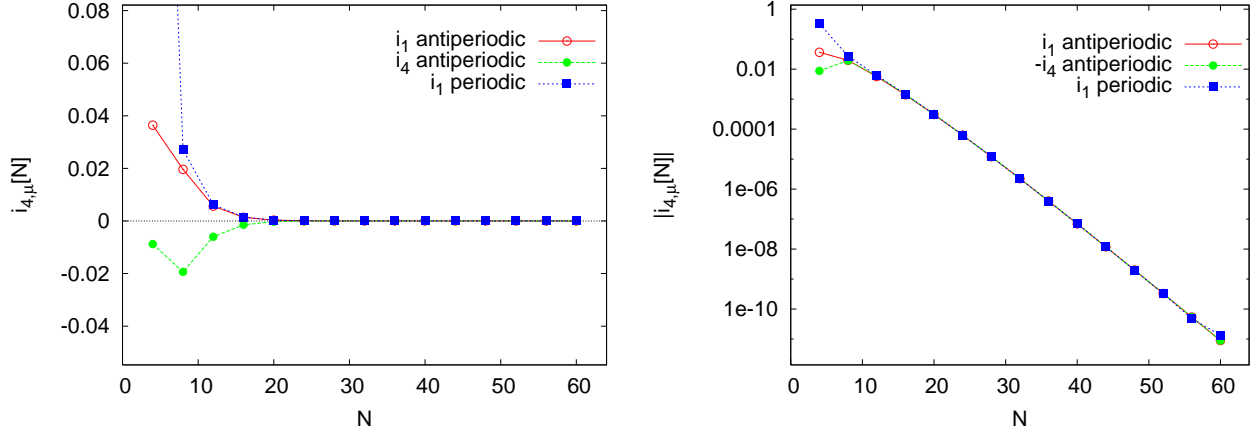


Figure 2: Riemann sums for coefficients  $i_{4,\mu}$  of Eq. (42). These results were computed at  $r = 1$  and  $\kappa = 0.19$  ( $\rho = 26/19$ ).

an additional check on our results. In what follows, we will refer to the discretization defined by Eq. (40) as *antiperiodic*, while the discretization where

$$k_\mu = (\delta k) l_\mu \quad \mu = 1, 2, 3, 4 \quad l_\mu = 0, 1, \dots, N-1 \quad (47)$$

will be referred to as *periodic*. We emphasize that when we speak of periodic or antiperiodic case, we also imply that the corresponding reduction  $\hat{c}(n) \rightarrow c(n)$  has been performed in a manner that is consistent with the remnant symmetries of the Riemann sum used. More precisely, for the periodic discretization the Riemann sums  $I(j, n)[N]$  are completely symmetric with respect to indices  $n_\mu$  and the reduction is thus as described in previous paragraph. However, for the antiperiodic case the Riemann sum is only symmetric with respect to exchange of spatial components  $n_1, n_2$  and  $n_3$ , and one thus has to keep track of larger set of coefficients  $c(n)$ . It is only with this prescription that the exact correspondence between the finite and infinite volume situations is realized in case of antiperiodic discretization of the integral. One implication of this is that, for antiperiodic case at finite  $N$ , the time-like components of vectors and tensors will not be exactly equal to space-like components. However, the difference (and recovery of full hypercubic symmetries of the infinite lattice) has to take place in the  $N \rightarrow \infty$  limit. In what follows, we will show results for both types of discretization. Perfect agreement has always been found as expected, and we thus provide the list of reduced coefficients  $c(n)$  of the periodic case only, which is more economic.

### 3.4.1 The Results

The first group of terms in Eq. (42) is not gauge invariant and so constants  $i_{4,\mu}$  are expected to be zero. We have numerically evaluated these constants using the result for corresponding coefficients  $c(n)$  obtained from *Mathematica*. Fig. 2 shows the typical convergence of the associated Riemann sums  $i_{4,\mu}[N]$  both in antiperiodic and periodic discretizations. For antiperiodic case both the time-like and the space-like case is shown to see that they are different at finite  $N$ . For  $N \rightarrow \infty$  all three sequences are expected to approach the common limit which is apparently zero in this case. The convergence is again exponential in  $N$ .

The second and the third group of terms contain combinations that appear in  $(\mu, \nu \text{ fixed})$

$$\text{tr}_c F_{\mu\nu} F_{\mu\nu} = -\text{tr}_c [A_\mu, A_\nu][A_\mu, A_\nu] = 2 \text{tr}_c (A_\mu A_\mu A_\nu A_\nu - A_\mu A_\nu A_\mu A_\nu) \quad (48)$$

and thus, in light of Conjecture 1, we anticipate that  $\beta_{\mu\nu} = -\alpha_{\mu\nu}$ . Also, due to hypercubic symmetries we must have that  $\alpha_{\mu\nu} \equiv \alpha$  and  $\beta_{\mu\nu} \equiv \beta$  are independent of  $\mu \neq \nu$ . Since our results were obtained using a symbolic algebra software, verifying these relations is not only a consistency check for the expected result, but also an internal check of our programs.

The set of reduced coefficients specifying constants  $\alpha_{\mu\nu}$  and  $\beta_{\mu\nu}$  are given in Tables 1 and 2 respectively ( $j = 9/2$ ). In Fig. 3 (top) we show the typical convergence of Riemann sums for  $\alpha_{\mu\nu}$  in both periodic and antiperiodic discretizations of the integral. For periodic case only  $\alpha_{12}$  is shown since full hypercubic symmetry in this case guarantees that, even at finite  $N$ ,  $\alpha_{\mu\nu}[N]$  is independent of  $\mu, \nu$ . Our results, obtained using symbolic algebra software, indeed comply with this. In the antiperiodic case we show both the representative of space–space combination ( $\alpha_{12}$ ) and the representative of space–time combination ( $\alpha_{14}$ ). All other possibilities for space–space and space–time combinations are exactly the same as the ones shown (even at finite  $N$ ) as expected from the restricted hypercubic symmetry. The convergence of the three Riemann sums is exponential, as was in all the previous cases, and the insert shows that they approach a common non–zero limit whose value  $\alpha$  can be easily extracted. The analogous results in case of  $\beta_{\mu\nu}$  are shown in the bottom plot of Fig. 3, and one can immediately see that, indeed,  $\beta = -\alpha$ .

Combining all the results for the scalar spinorial component of  $D_{0,0}$  together, we have from Eq. (41) that

$$\text{tr}_{sc} D_{0,0}(U(a)) = \text{tr}_{sc} D_{0,0}(\mathbb{I}) + a^4 \frac{\alpha}{4} \sum_{\mu\nu} \text{tr}_c F_{\mu\nu} F_{\mu\nu} + \mathcal{O}(a^6) \quad (49)$$

implying that Conjecture 1 (see Eq.(7)) is indeed true for the class of constant fields. The associated proportionality constant is given by

$$c^S(\rho, r) = \frac{\alpha(\rho, r)}{4} \quad \longrightarrow \quad c^S\left(\frac{26}{19}, 1\right) = 0.01672926781 \quad (50)$$

where the quoted value at  $\rho = 26/19$  and  $r = 1$  (only valid digits are given) was extracted from the data shown in Fig. 3.

## 4 Finite Volume and Non–Constant Fields

As already mentioned in the previous section, we have analyzed the case of constant fields in the infinite volume in a way that can be directly mapped on to the situation in finite volume with specific boundary conditions. We now discuss this correspondence explicitly. Consider a 4–d hypercube in the continuum with side  $L_p$  (in physical units). Superimposing a hypercubic lattice with  $N^4$  sites implies the classical lattice spacing  $a \equiv a_N$  such that

$$L_p = N a_N \quad (51)$$

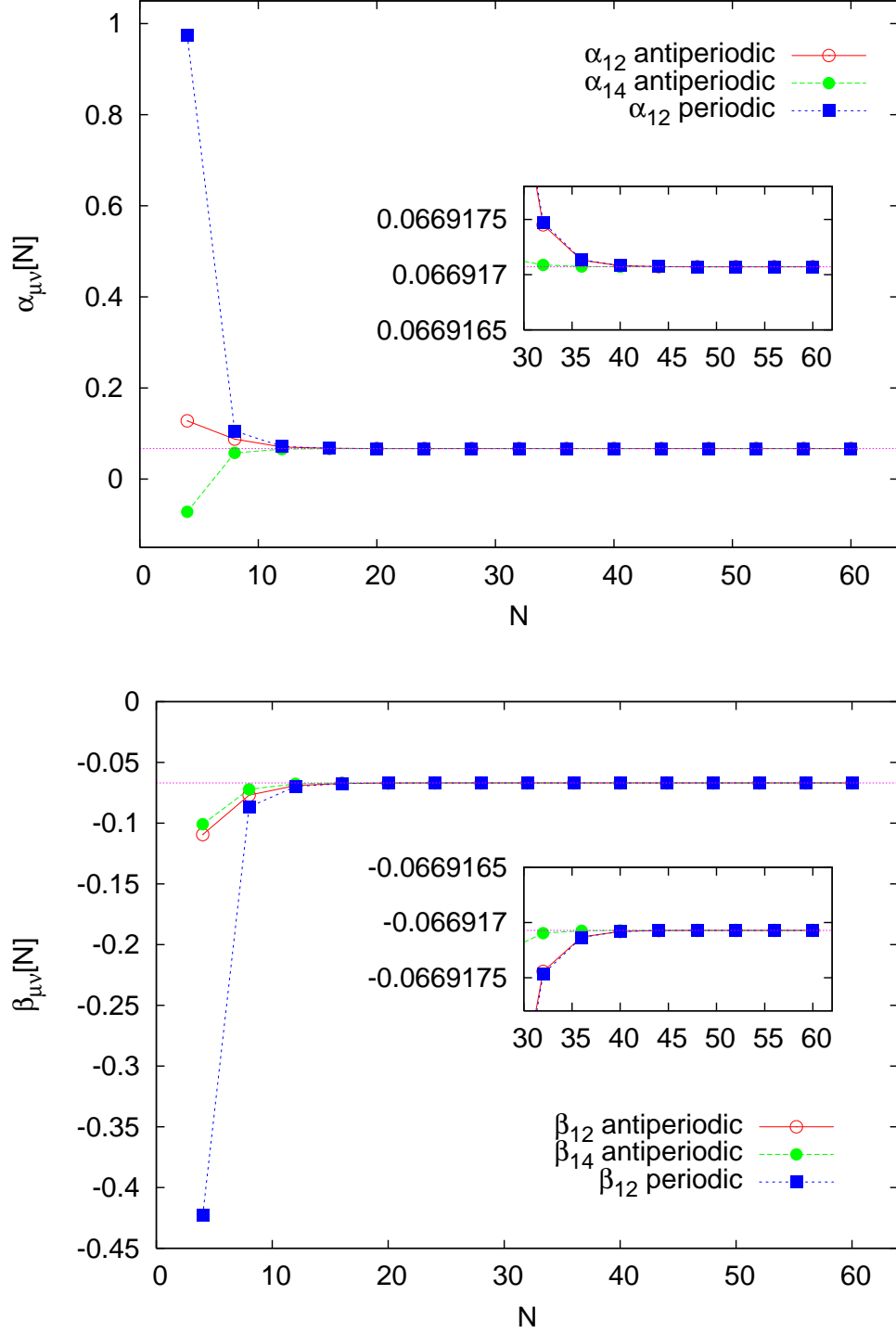


Figure 3: Riemann sums for constants  $\alpha_{\mu\nu}$  (top) and  $\beta_{\mu\nu}$  (bottom) of the scalar term (see Eq. (42)). These results were computed at  $r = 1$  and  $\kappa = 0.19$  ( $\rho = 26/19$ ).

and the classical continuum limit is achieved as  $N \rightarrow \infty$  ( $a_N \rightarrow 0$ ). Proper specification of the operator now involves also a choice of boundary conditions, and we will consider (see below) two standard cases that admit a diagonal Fourier-space representation for constant fields. In particular, we will refer to the situation with periodic boundary conditions in all directions as “periodic bc”, and to the case with periodic boundary conditions in spatial ( $\mu = 1, 2, 3$ ) directions and antiperiodic in time ( $\mu = 4$ ) as “antiperiodic bc”. The formulas (10) relating the direct and Fourier representations carry over to these finite volume cases except that the infinite sum is replaced by the finite sum, and the integral of the inverse transform is replaced by

$$O_{n,m} = \frac{1}{(2\pi)^4} \int d^4k e^{i(n-m)k} O(k) \quad \longrightarrow \quad O_{n,m} = \frac{1}{N^4} \sum_k e^{i(n-m)k} O(k) \quad (52)$$

with sum only running over the associated  $N^4$  discrete momenta.

The relation to the infinite-volume case is based on the following considerations.

(i) With periodic bc, the  $N^4$ -dimensional Fourier space is spanned by plane waves with momenta given by Eq. (47), namely those involved in the periodic discretization (into  $N^4$  pieces) of the Brillouin zone discussed in case of infinite volume. Similarly, for antiperiodic bc the associated momenta are given by Eq. (40) of the antiperiodic discretization.

(ii) The form of Fourier representation  $D(k)$  of the overlap operator for the above finite volume setups (and constant fields) is identical to the infinite volume case but restricted to the corresponding discrete momenta.

(iii) Using (i), (ii) and comparing (52) with the rule for evaluating Riemann sums in case of infinite volume (see e.g. Eq. (39)) we can immediately see the following correspondence

$$D_{0,0}^{fin}(a, N) \equiv D_{0,0}^{inf}(a)[N] \quad (53)$$

where the superscripts “inf” and “fin” refer to infinite and finite volume cases respectively. In other words, the matrix  $D_{0,0}^{fin}(a, N)$  (for finite volume setups discussed here) is equal to the corresponding Riemann sum (with  $N^4$  terms) for the inverse Fourier transform representation of  $D_{0,0}^{inf}(a)$ . The same constant background is of course implicitly assumed in both cases.

(iv) Riemann sums in question converge exponentially in  $N$ , as emphasized in previous sections, and we can conclude from (53) that for large  $N$

$$D_{0,0}^{fin}(a, N) = D_{0,0}^{inf}(a) + \mathcal{O}\left(\exp(-C(a)N)\right) \quad (54)$$

with strictly positive  $C(a)$  (also at  $a = 0$ ).

From the last equation it follows that, in the case of constant background fields, the Taylor expansion (in  $a$ ) of  $D_{0,0}$  in infinite volume supplies an asymptotic expansion for the case of finite volume (with corections behaving as  $\exp(-C(a)L_p/a)$ ). Moreover, considering the continuum limit at fixed  $L_p$  (so that  $a_N \equiv L_p/N$ ) we obtain that

$$\lim_{N \rightarrow \infty} \frac{\text{tr}_{sc} \left( D_{0,0}^{fin}(a_N, N) - D_{0,0}^{fin}(0, N) \right)}{a_N^4 \text{tr}_c F_{\mu\nu} F_{\mu\nu}} = \lim_{N \rightarrow \infty} \frac{\text{tr}_{sc} \left( D_{0,0}^{inf}(a_N) - D_{0,0}^{inf}(0) \right)}{a_N^4 \text{tr}_c F_{\mu\nu} F_{\mu\nu}} \equiv c^S \quad (55)$$

where  $c^S$  is the constant that we computed in the infinite volume. The above equation expresses the fact that the scalar component of  $D_{0,0}$  has the same classical limit in both finite and infinite volumes, as required and expected on the basis of locality. Analogous result obviously holds also for the tensor component.

## 4.1 Non-Constant Fields

Apart from the fact that the finite-volume setups are actually those relevant for practical lattice QCD calculations, their advantage for the present discussion is that one can evaluate the associated classical limit numerically. In other words, one can obtain the left-hand side of Eq. (55) via direct numerical evaluation of  $D_{0,0}^{fin}$  for *arbitrary* classical background. Performing a sequence of such calculations with increasing  $N$  then allows us to infer the  $N \rightarrow \infty$  ( $a_N \rightarrow 0$ ) limit of the ratio. For the case of constant fields, such calculations indeed exactly reproduce our results obtained via the expansion in classical lattice spacing. The utility of this approach however mainly lies in the fact that it allows us to evaluate classical limits also for non-constant backgrounds which were not included in our considerations up to this point.

To perform such a calculation, we set  $L_p = 1$  and use arbitrarily selected classical backgrounds. One of the cases that we studied is specified by

$$A_\mu(t, x, y, z) = \left(1 + \frac{\sin 2\pi t \cos 2\pi x \mu}{12\pi}\right) a_\mu + \left(1 + \frac{\cos 2\pi z}{2\pi}\right) a_{3-\mu} \quad (56)$$

where we use  $\mu \in \{0, 1, 2, 3\}$  and the coordinate-labeling correspondence  $0 \leftrightarrow t$ ,  $1 \leftrightarrow x$ ,  $2 \leftrightarrow y$ ,  $3 \leftrightarrow z$  for convenience. The constant field  $a_\mu$  is specified in Appendix C.

For given  $N$ , we evaluated the ratio  $c^S(N = 1/a_N)$  at 10 randomly selected points on the unit torus. The same points, specified in Appendix C, were used for each  $N$ . In Fig. 4 (top) we plot the mean value of  $c^S(N)$  over this sample with “error bars” representing the square root of the associated variance. The horizontal line shows the value of  $c^S$  obtained via expansion in classical lattice spacing in infinite volume (50). As can be seen quite clearly, the mean approaches this predicted value for large  $N$  with variance shrinking toward zero at the same time. To guide the eye, we also included a fit to  $N = 1/a_N$  dependence of  $c^S$  in the form

$$c^S(N) = \sum_{k=0}^K c_k \left(\frac{1}{N}\right)^{2k} \quad (57)$$

Note that this form is motivated by the fact that the odd powers of lattice spacing are not present in the expansion of  $D_{0,0}$  in infinite volume. The above fitting form is neglecting the terms exponentially small in  $N$ , which are present, but their relative contribution decays very fast with increasing  $N$ . The standard fit shown in Fig. 4 uses all points with  $N \geq 12$  (treating the associated rooted variances as error bars) and  $K = 6$ . The coefficient  $c_0$  of the fit represents the estimate of  $c^S$ , and the obtained value agrees with that of Eq. (50) to relative precision of about two parts in  $10^4$ .

To further check the robustness of the agreement found above (universality of the classical limit for constant and non-constant configurations), let us now examine a different procedure for estimating  $c^S$  on background (56). For any given point on the torus, consider evaluating

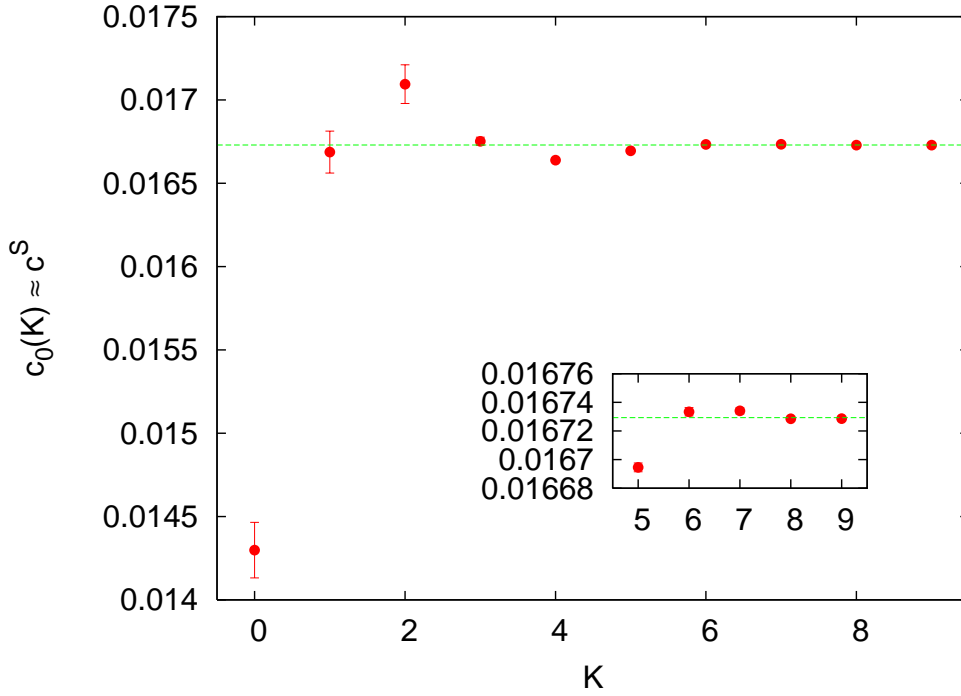
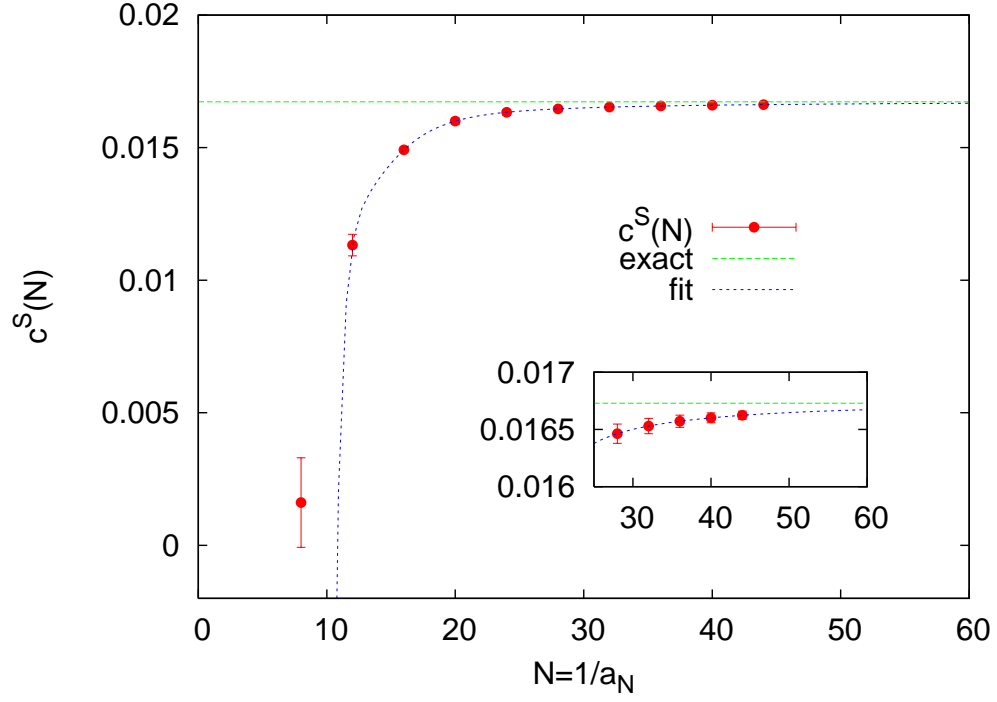


Figure 4: Evaluation of classical limit on a finite torus ( $L_p = 1$ ) for non-constant background field (56). The meaning of the data is explained in the text. The overlap operator used is specified by  $r = 1$  and  $\kappa = 0.19$  ( $\rho = 26/19$ ).



the ratio (55) over some range of  $N$  (such as one shown in Fig. 4 (top)), and then fitting this dependence to the form (57) with progressively increasing value of  $K$ .<sup>10</sup> For each  $K$ , the coefficient  $c_0 \equiv c_0(K)$  of the fit represents the estimate of  $c^S$ . Since the expansion (57) is asymptotically valid at large values of  $N$ , the accuracy of such estimates will depend on the fitting range chosen. In order to be very conservative, we use the whole range displayed in Fig. 4 (top), i.e. all the points with  $8 \leq N \leq 44$ . In Fig. 4 (bottom) we show the average of  $c_0(K)$  so obtained over the same sample of random points that we used above. The “errorbars” on this plot are the square roots of variance over this sample, and are decaying rapidly with increasing  $K$ . This is expected since the classical limit has to be reproduced at each point individually and the estimates are expected to get better with increasing  $K$ . The horizontal line on the plot represents the value of  $c^S$  quoted in Eq. (50). As one can see quite clearly,  $c_0(K)$  settles approximately at this expected value. In fact, for the largest value of  $K$  ( $K = 9$ ) the relative difference between  $c^S$  and  $c_0$  is about three parts in  $10^5$ .

## 5 Values of Related Constants

Given the results presented in Secs. 3, 4 there is little doubt that the universal classical limit for the scalar spinorial part of  $D_{0,0}$  exists in the case of overlap operator, and that it is proportional to  $F_{\mu\nu}(0)F_{\mu\nu}(0)$  [1]. Indeed, we obtained fully consistent results showing this for finite and infinite volumes, for constant and non-constant fields, and for different boundary conditions in finite volume. Since matrix elements of  $D$  are local functions of the gauge field [5], the lattice operator

$$O(n, U) \equiv \frac{1}{c^S} \text{tr}_{sc} \left( D_{n,n}(U) - D_{n,n}(\mathbb{I}) \right) \quad (58)$$

represents a valid definition of  $\text{tr}_c F_{\mu\nu} F_{\mu\nu}$ . For certain applications, such as those arising in the studies of QCD vacuum structure, it is necessary to deal with properly normalized operators in which case it is important that sufficiently precise values of  $c^S$  and free-field subtraction constants are available. In this section, we provide some of this information both for the scalar and tensor cases.

As is well known, the properties of the overlap Dirac operator, such as its range of locality [5], are quite sensitive to the value of the negative mass parameter  $\rho$ . Since various choices are currently being used in practice, we computed  $c^S(\rho, r)$  and  $c^T(\rho, r)$  for the range of  $\rho$ -values and the most commonly used case of  $r = 1$ . To obtain the results listed in Table 3, we used the expansion method described in Sec. 3. The last column lists the maximal discretization parameter  $N$  used in evaluating the associated Riemann sums. Note that one needs to use finer discretization (larger  $N$ ) close to boundary values  $\rho = 0$  and  $\rho = 2$  to achieve given precision.

In Figure 5, we plot the  $\rho$ -dependence of both  $c^S/\rho$  and  $c^T/\rho$ . It is worth pointing out that in the tensor case the behavior appears to be almost exactly linear in  $\rho$ . However, closer inspection suggests that the deviations from exact linearity are in fact larger than the

---

<sup>10</sup>Note that all the points in the chosen range contribute with equal weight in such fit – there are no errorbars. Indeed, classical limit is not a “statistical” notion and has to be consistently reproduced at all non-singular points and for all classical configurations.

$\rho$	$\kappa$	$c^S/\rho$	$c^T/\rho$	max $N$
0.2	0.131579	$7.2764827 \times 10^{-3}$	$2.30823770 \times 10^{-2}$	160
0.3	0.135135	$7.2792339 \times 10^{-3}$	$2.78332999 \times 10^{-2}$	120
0.4	0.138889	$7.3198516 \times 10^{-3}$	$3.26397580 \times 10^{-2}$	100
0.5	0.142857	$7.4053234 \times 10^{-3}$	$3.75015319 \times 10^{-2}$	100
0.6	0.147059	$7.5441944 \times 10^{-3}$	$4.24178729 \times 10^{-2}$	80
0.7	0.151515	$7.7470040 \times 10^{-3}$	$4.73873153 \times 10^{-2}$	80
0.8	0.156250	$8.0268757 \times 10^{-3}$	$5.24074212 \times 10^{-2}$	80
0.9	0.161290	$8.4003244 \times 10^{-3}$	$5.74744291 \times 10^{-2}$	80
1.0	0.166667	$8.8883824 \times 10^{-3}$	$6.25827634 \times 10^{-2}$	80
1.1	0.172414	$9.5181966 \times 10^{-3}$	$6.77243431 \times 10^{-2}$	80
1.2	0.178571	$1.0325346 \times 10^{-2}$	$7.28875894 \times 10^{-2}$	80
1.3	0.185185	$1.1357281 \times 10^{-2}$	$7.80559770 \times 10^{-2}$	80
1.4	0.192308	$1.2678582 \times 10^{-2}$	$8.32058759 \times 10^{-2}$	80
1.5	0.200000	$1.4379234 \times 10^{-2}$	$8.83032584 \times 10^{-2}$	100
1.6	0.208333	$1.6588164 \times 10^{-2}$	$9.32985300 \times 10^{-2}$	120
1.7	0.217391	$1.9496369 \times 10^{-2}$	$9.81181443 \times 10^{-2}$	120
1.8	0.227273	$2.3398534 \times 10^{-2}$	$1.02650441 \times 10^{-1}$	180

Table 3: The proportionality constants  $c^S$  and  $c^T$  for various values of  $\rho$  at  $r = 1$ .

estimated errors of calculated values. Nevertheless, the purely linear approximation is very precise in the range of  $\rho$ -values studied.

Finally, we have computed the subtraction constants  $\text{tr}_{sc} D_{0,0}(\mathbb{I})$  for various sizes of a symmetric lattice with both periodic and antiperiodic boundary conditions. The results, summarized in Table 4, were computed at  $\rho = 26/19$  and  $r = 1$ . These are the values of the parameters used by the Kentucky group in the studies of QCD vacuum structure (see e.g. [7, 13, 21]) as well as in the studies of hadron spectroscopy (see e.g. [25, 26]). In the space-time symmetric geometry considered here, the utility of these results is mainly for the former. To obtain the constants quoted in Table 4, we directly evaluated  $\text{tr}_{sc} D_{0,0}(\mathbb{I})$  from the finite spectral sum over explicitly available Fourier modes. The calculation was done in double precision and we estimate that after rounding errors, these values are good to at least thirteen digits. Note that the convergence to the infinite volume value is very fast and that at  $N = 40$  the periodic and the antiperiodic cases already agree to 13 digits.

## 6 Summary

We have used analytic and numerical techniques to evaluate the classical limit of the gauge operator  $\text{tr}_{sc} D_{0,0}(U)$  with  $D \equiv D^{(\rho,r)}$  being the overlap Dirac matrix.<sup>11</sup> As suggested on general grounds [1], we found that the limit is proportional to  $\text{tr}_c F_{\mu\nu}(0)F_{\mu\nu}(0)$  of the

<sup>11</sup>All the results presented in this manuscript were obtained in the Summer of 2006 and were partially discussed by the second author in Lattice 2006 talk that focused on coherent LQCD. In the Summer of 2007 we were informed by David Adams [20] that he has just computed the constant  $c^S(\rho, r)$  as well. His approach leads to an integral expression with integrand different from ours, but yielding identical final answers after

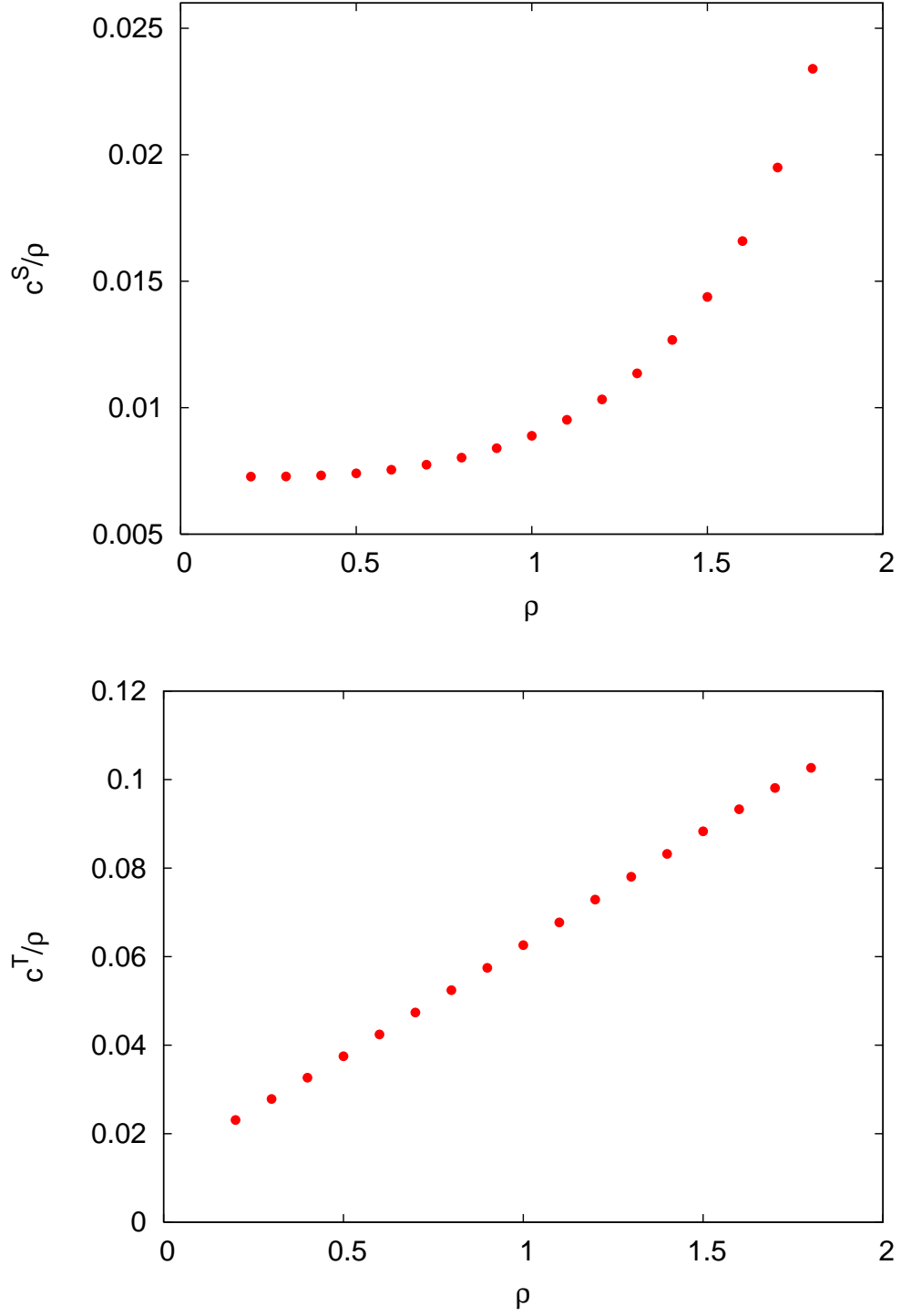


Figure 5: Dependence of rescaled constants  $c^S$  (top) and  $c^T$  (bottom) on the negative mass parameter  $\rho$  at  $r = 1$ .

$N$	periodic bc	antiperiodic bc
04	21.4358235894802	21.4010898463124
08	21.3940949198520	21.3935062781772
12	21.3931417096880	21.3931106079229
16	21.3930879676987	21.3930856400191
20	21.3930838480598	21.3930836424736
24	21.3930834815890	21.3930834616044
28	21.3930834459514	21.3930834438807
32	21.3930834422695	21.3930834420471
36	21.3930834418726	21.3930834418505
40	21.3930834418356	21.3930834418306

Table 4: The subtraction constants  $\text{tr}_{sc} D_{0,0}(\mathbb{I})$  on  $N^4$  lattice with periodic and antiperiodic (in time) boundary conditions. These results were calculated at  $\rho = 26/19$  and  $r = 1$ .

associated classical background after the subtraction of the free-field constant. Accordingly, the version of coherent LQCD where  $\text{Tr } D(U)$  serves as a basis for the gauge action [1] represents a valid regularization of QCD. In addition, this operator is expected to be useful as a natural partner to the overlap-based definition of pseudoscalar (topological) density both in studies of QCD vacuum structure and in standard applications of hadronic physics (such as calculations of glueball masses). In the former case it is of interest to explore the relation between the fundamental structure seen in topological density [12, 13, 21, 22, 23, 24], and the structure in scalar density that is expected to be visible if the overlap-based definition (58) is used.

Techniques used here for the scalar case were applied in parallel also to the tensor component of  $D_{0,0}$ . In our previous work [17] we have explicitly derived this classical limit (proportional to  $F_{\mu\nu}(0)$ ) in a general setting, and the complete agreement found in this work serves as a valuable cross-check for both types of calculations.

With possible practical applications in mind, we have computed the proportionality constants  $c^S$  and  $c^T$  for a wide range of negative mass parameter  $\rho$ . One notable feature of the  $\rho$ -dependence found is that  $c^T(\rho)/\rho$  is surprisingly well described by a purely linear behavior in the region  $0.2 \leq \rho \leq 1.8$ .

---

integration. We hope that his derivation will be publicly available in due course.

## A Alternative derivation to second order

The expansion of the overlap operator for constant fields to the second order in the lattice spacing can be simplified as follows. We start by noticing that

$$\begin{aligned}\lim_{a \rightarrow 0} \frac{\partial^n}{\partial a^n} X &= \left( \sum_{\mu} A_{\mu} \frac{\partial}{\partial k_{\mu}} \right)^n X_0, \\ \lim_{a \rightarrow 0} \frac{\partial}{\partial a} B &= \sum_{\mu} A_{\mu} \frac{\partial}{\partial k_{\mu}} B_0, \\ \lim_{a \rightarrow 0} \frac{\partial^2}{\partial a^2} B &= \left( \sum_{\mu} A_{\mu} \frac{\partial}{\partial k_{\mu}} \right)^2 B_0 + \delta_2,\end{aligned}\tag{59}$$

where

$$\delta_2 = \frac{1}{2} \sum_{\mu, \nu} [A_{\mu}, A_{\nu}] \left( \frac{\partial X_0^{\dagger}}{\partial k_{\mu}} \frac{\partial X_0}{\partial k_{\nu}} - \frac{\partial X_0^{\dagger}}{\partial k_{\nu}} \frac{\partial X_0}{\partial k_{\mu}} \right)\tag{60}$$

Using the above formulas and the straightforward algebra one can show that

$$\begin{aligned}\lim_{a \rightarrow 0} \frac{\partial}{\partial a} \frac{1}{\rho} D &= \sum_{\mu} A_{\mu} \frac{\partial}{\partial k_{\mu}} X_0 B_0^{-1/2}, \\ \lim_{a \rightarrow 0} \frac{\partial^2}{\partial a^2} \frac{1}{\rho} D &= \left( \sum_{\mu} A_{\mu} \frac{\partial}{\partial k_{\mu}} \right)^2 X_0 B_0^{-1/2} - \frac{1}{2} X_0 B_0^{-3/2} \delta_2\end{aligned}\tag{61}$$

The derivative terms  $\sum_{\mu} A_{\mu} \frac{\partial}{\partial k_{\mu}} f(k)$  vanish upon momentum integration and we have

$$\frac{1}{\rho} D_{0,0}(U(a)) = \frac{1}{\rho} D_{0,0}(\mathbb{I}) + \frac{a^2}{2} \frac{1}{(2\pi)^4} \int d^4 k \left( -\frac{1}{2} X_0 B_0^{-3/2} \delta_2 \right) + \mathcal{O}(a^3)\tag{62}$$

After expanding  $\delta_2$  and dropping the terms odd in  $k_{\mu}$  we get

$$\frac{1}{\rho} D_{0,0}(U(a)) = \frac{1}{\rho} D_{0,0}(\mathbb{I}) + \frac{a^2}{2} \frac{r}{(4r - \rho)^3} \sum_{\mu\nu} \sigma_{\mu\nu} \times F_{\mu\nu} \frac{1}{(2\pi)^4} \int d^4 k \frac{t_{\mu\nu}(k)}{B_0^{3/2}(k)} + \mathcal{O}(a^3)\tag{63}$$

with  $t_{\mu\nu}$  defined in Eq. (32).

## B Reduced Coefficients

The tables in this Appendix specify the reduced coefficients  $c(n)$  and powers  $j$  defining (via Eq. (46)) various constants appearing in the expansion of the scalar part of  $D_{0,0}$  in classical lattice spacing. As discussed in Secs. 3.4 and 4, these coefficients can also be used for evaluation of corresponding constants on a finite symmetric torus with periodic boundary conditions in all directions.

$n_1$	$n_2$	$n_3$	$n_4$	$c(n)/\rho$
0	0	0	0	$48\kappa^4 + 192r^2\kappa^4 + 1536\kappa^6 - 1536r^2\kappa^6 - 10240r^4\kappa^6 + 12288\kappa^8 - 73728r^2\kappa^8 + 122880r^4\kappa^8$
1	0	0	0	$-32r\kappa^3 - 1152r\kappa^5 - 2560r^3\kappa^5 - 18432r\kappa^7 - 24576r^3\kappa^7 + 245760r^5\kappa^7 - 131072r\kappa^9 + 589824r^3\kappa^9 - 983040r^5\kappa^9$
1	1	0	0	$576r^2\kappa^4 + 12416r^2\kappa^6 - 30720r^4\kappa^6 - 14336r^2\kappa^8 + 516096r^4\kappa^8 - 1474560r^6\kappa^8$
1	1	1	0	$-75264r^3\kappa^7 + 368640r^5\kappa^7 + 204800r^3\kappa^9 - 1179648r^5\kappa^9 + 1966080r^7\kappa^9$
1	1	1	1	$-15360r^4\kappa^6 + 132096r^4\kappa^8 - 614400r^6\kappa^8$
2	0	0	0	$-192\kappa^4 - 96r^2\kappa^4 - 5760\kappa^6 + 15232r^2\kappa^6 + 20480r^4\kappa^6 - 43008\kappa^8 + 321536r^2\kappa^8 - 319488r^4\kappa^8 - 491520r^6\kappa^8$
2	1	0	0	$64r\kappa^3 + 4032r\kappa^5 + 1216r^3\kappa^5 + 74496r\kappa^7 - 232704r^3\kappa^7 + 290816r\kappa^9 - 1503232r^3\kappa^9 + 1179648r^5\kappa^9 + 2949120r^7\kappa^9$
2	1	1	0	$-1440r^2\kappa^4 - 13824r^2\kappa^6 - 42496r^4\kappa^6 - 198656r^2\kappa^8 + 952320r^4\kappa^8 - 1474560r^6\kappa^8$
2	1	1	1	$6720r^3\kappa^5 - 18432r^3\kappa^7 + 242688r^5\kappa^7 + 77824r^3\kappa^9 - 774144r^5\kappa^9 + 1966080r^7\kappa^9$
2	2	0	0	$240\kappa^4 - 480r^2\kappa^4 + 8448\kappa^6 - 25600r^2\kappa^6 - 23808r^4\kappa^6 + 77824\kappa^8 - 561152r^2\kappa^8 + 861696r^4\kappa^8 + 184320r^6\kappa^8$
2	2	1	0	$-5568r\kappa^5 + 16896r^3\kappa^5 - 78336r\kappa^7 + 170496r^3\kappa^7 + 344064r^5\kappa^7 - 282624r\kappa^9 + 1835008r^3\kappa^9 - 3336192r^5\kappa^9 + 737280r^7\kappa^9$
2	2	1	1	$24576r^2\kappa^6 - 92928r^4\kappa^6 + 110592r^2\kappa^8 - 12288r^4\kappa^8 - 1081344r^6\kappa^8$
2	2	2	0	$-3840\kappa^6 + 28416r^2\kappa^6 - 37888r^4\kappa^6 - 49152\kappa^8 + 338944r^2\kappa^8 - 448512r^4\kappa^8 - 433152r^6\kappa^8$
2	2	2	1	$23040r\kappa^7 - 184320r^3\kappa^7 + 310272r^5\kappa^7 + 73728r\kappa^9 - 518144r^3\kappa^9 + 516096r^5\kappa^9 + 1075200r^7\kappa^9$
2	2	2	2	$7680\kappa^8 - 67584r^2\kappa^8 + 241152r^4\kappa^8 - 224256r^6\kappa^8$
3	0	0	0	$576r\kappa^5 + 64r^3\kappa^5 + 11520r\kappa^7 + 25344r^3\kappa^7 - 122880r^5\kappa^7 + 184320r\kappa^9 - 765952r^3\kappa^9 + 786432r^5\kappa^9 + 327680r^7\kappa^9$
3	1	0	0	$-288r^2\kappa^4 - 20224r^2\kappa^6 + 27136r^4\kappa^6 + 38912r^2\kappa^8 - 509952r^4\kappa^8 + 983040r^6\kappa^8$
3	1	1	0	$4800r^3\kappa^5 + 132096r^3\kappa^7 - 242688r^5\kappa^7 - 397312r^3\kappa^9 + 1306624r^5\kappa^9 - 983040r^7\kappa^9$
3	1	1	1	$-15360r^4\kappa^6 - 153600r^4\kappa^8 + 307200r^6\kappa^8$
3	2	0	0	$-2112r\kappa^5 + 3776r^3\kappa^5 - 69888r\kappa^7 + 116736r^3\kappa^7 + 76800r^5\kappa^7 - 540672r\kappa^9 + 1982464r^3\kappa^9 - 1628160r^5\kappa^9 - 1228800r^7\kappa^9$
3	2	1	0	$44544r^2\kappa^6 - 105472r^4\kappa^6 + 409600r^2\kappa^8 - 657408r^4\kappa^8 - 188416r^6\kappa^8$
3	2	1	1	$-156672r^3\kappa^7 + 420864r^5\kappa^7 - 260096r^3\kappa^9 + 233472r^5\kappa^9 + 131072r^7\kappa^9$
3	2	2	0	$50688r\kappa^7 - 238080r^3\kappa^7 + 258048r^5\kappa^7 + 432128r\kappa^9 - 1789952r^3\kappa^9 + 1687552r^5\kappa^9 + 792576r^7\kappa^9$
3	2	2	1	$-211968r^2\kappa^8 + 1069056r^4\kappa^8 - 1422336r^6\kappa^8$
3	2	2	2	$-73728r\kappa^9 + 430080r^3\kappa^9 - 964608r^5\kappa^9 + 665600r^7\kappa^9$
3	3	0	0	$8576r^2\kappa^6 - 11008r^4\kappa^6 - 18432r^2\kappa^8 + 132096r^4\kappa^8 - 184320r^6\kappa^8$
3	3	1	0	$-130560r^3\kappa^7 + 205824r^5\kappa^7 + 188416r^3\kappa^9 - 634880r^5\kappa^9 + 401408r^7\kappa^9$
3	3	1	1	$297984r^4\kappa^8 - 528384r^6\kappa^8$
3	3	2	0	$-100352r^2\kappa^8 + 482304r^4\kappa^8 - 496640r^6\kappa^8$
3	3	2	1	$237568r^3\kappa^9 - 1124352r^5\kappa^9 + 1382400r^7\kappa^9$
3	3	3	0	$-20480r^3\kappa^9 - 75776r^5\kappa^9 + 133120r^7\kappa^9$

Table 1 (part 1). Coefficients  $c(n)$  for constants  $\alpha_{\mu\nu}$  of Eq. (42). In this case  $j = 9/2$ .

$n_1$	$n_2$	$n_3$	$n_4$	$c(n)/\rho$
4	0	0	0	$-384\kappa^6 - 3328r^2\kappa^6 + 3328r^4\kappa^6 - 10752\kappa^8 - 28672r^2\kappa^8 - 109056r^4\kappa^8 + 266240r^6\kappa^8$
4	1	0	0	$384r\kappa^5 - 192r^3\kappa^5 - 3072r\kappa^7 + 140544r^3\kappa^7 - 168960r^5\kappa^7 + 111616r\kappa^9 - 188416r^3\kappa^9 + 885760r^5\kappa^9 - 1351680r^7\kappa^9$
4	1	1	0	$-6912r^2\kappa^6 + 6912r^4\kappa^6 + 52224r^2\kappa^8 - 829440r^4\kappa^8 + 1019904r^6\kappa^8$
4	1	1	1	$23040r^3\kappa^7 - 32256r^5\kappa^7 - 61440r^3\kappa^9 + 694272r^5\kappa^9 - 847872r^7\kappa^9$
4	2	0	0	$2176r^2\kappa^6 - 3072r^4\kappa^6 - 9728\kappa^8 + 251904r^2\kappa^8 - 430080r^4\kappa^8 + 64000r^6\kappa^8$
4	2	1	0	$-4608r\kappa^7 - 39936r^3\kappa^7 + 70656r^5\kappa^7 - 26624r\kappa^9 - 770048r^3\kappa^9 + 2027520r^5\kappa^9 - 997376r^7\kappa^9$
4	2	1	1	$23040r^2\kappa^8 + 79872r^4\kappa^8 - 155136r^6\kappa^8$
4	2	2	0	$7680\kappa^8 - 117760r^2\kappa^8 + 290304r^4\kappa^8 - 156672r^6\kappa^8$
4	2	2	1	$3072r\kappa^9 + 180224r^3\kappa^9 - 654336r^5\kappa^9 + 460800r^7\kappa^9$
4	3	0	0	$19200r\kappa^7 - 68352r^3\kappa^7 + 52224r^5\kappa^7 + 10240r\kappa^9 - 33792r^3\kappa^9 - 182272r^5\kappa^9 + 332800r^7\kappa^9$
4	3	1	0	$-144384r^2\kappa^8 + 651264r^4\kappa^8 - 592896r^6\kappa^8$
4	3	1	1	$125952r^3\kappa^9 - 712704r^5\kappa^9 + 721920r^7\kappa^9$
4	3	2	0	$-38912r\kappa^9 + 417792r^3\kappa^9 - 950272r^5\kappa^9 + 563200r^7\kappa^9$
4	4	0	0	$10240\kappa^8 - 80384r^2\kappa^8 + 132096r^4\kappa^8 - 64512r^6\kappa^8$
4	4	1	0	$-34816r\kappa^9 + 303104r^3\kappa^9 - 595968r^5\kappa^9 + 337920r^7\kappa^9$
5	0	0	0	$6912r\kappa^7 - 768r^3\kappa^7 - 6144r^5\kappa^7 - 21504r\kappa^9 + 131072r^3\kappa^9 + 7168r^5\kappa^9 - 188416r^7\kappa^9$
5	1	0	0	$-3072r^2\kappa^6 + 2816r^4\kappa^6 - 25600r^2\kappa^8 - 181248r^4\kappa^8 + 237568r^6\kappa^8$
5	1	1	0	$41472r^3\kappa^7 - 41472r^5\kappa^7 - 63488r^3\kappa^9 + 706560r^5\kappa^9 - 765952r^7\kappa^9$
5	1	1	1	$-92160r^4\kappa^8 + 98304r^6\kappa^8$
5	2	0	0	$-9216r\kappa^7 + 21504r^3\kappa^7 - 10752r^5\kappa^7 + 115712r\kappa^9 - 458752r^3\kappa^9 + 489472r^5\kappa^9 - 64512r^7\kappa^9$
5	2	1	0	$64512r^2\kappa^8 - 196608r^4\kappa^8 + 107520r^6\kappa^8$
5	2	1	1	$-64512r^3\kappa^9 + 251904r^5\kappa^9 - 162816r^7\kappa^9$
5	2	2	0	$-52224r\kappa^9 + 137216r^3\kappa^9 - 58368r^5\kappa^9 - 49152r^7\kappa^9$
5	3	0	0	$-6656r^2\kappa^8 + 46080r^4\kappa^8 - 42496r^6\kappa^8$
5	3	1	0	$63488r^3\kappa^9 - 258048r^5\kappa^9 + 247808r^7\kappa^9$
5	4	0	0	$-41984r\kappa^9 + 156672r^3\kappa^9 - 189440r^5\kappa^9 + 76800r^7\kappa^9$
6	0	0	0	$4608\kappa^8 - 25600r^2\kappa^8 + 24576r^4\kappa^8 - 3584r^6\kappa^8$
6	1	0	0	$-2304r\kappa^7 + 6912r^3\kappa^7 - 4608r^5\kappa^7 - 35840r\kappa^9 + 112640r^3\kappa^9 - 10240r^5\kappa^9 - 66560r^7\kappa^9$
6	1	1	0	$19968r^2\kappa^8 - 64512r^4\kappa^8 + 44544r^6\kappa^8$
6	1	1	1	$-21504r^3\kappa^9 + 73728r^5\kappa^9 - 52224r^7\kappa^9$
6	2	0	0	$-7680\kappa^8 + 42496r^2\kappa^8 - 58368r^4\kappa^8 + 23552r^6\kappa^8$
6	2	1	0	$34816r\kappa^9 - 182272r^3\kappa^9 + 258048r^5\kappa^9 - 110592r^7\kappa^9$
6	3	0	0	$23552r\kappa^9 - 62464r^3\kappa^9 + 37888r^5\kappa^9 + 1024r^7\kappa^9$
7	0	0	0	$-4096r\kappa^9 + 17408r^3\kappa^9 - 22528r^5\kappa^9 + 9216r^7\kappa^9$
7	1	0	0	$1536r^2\kappa^8 - 3072r^4\kappa^8 + 1536r^6\kappa^8$
7	1	1	0	$-9216r^3\kappa^9 + 18432r^5\kappa^9 - 9216r^7\kappa^9$
7	2	0	0	$5120r\kappa^9 - 23552r^3\kappa^9 + 31744r^5\kappa^9 - 13312r^7\kappa^9$
8	1	0	0	$-1024r\kappa^9 + 3072r^3\kappa^9 - 3072r^5\kappa^9 + 1024r^7\kappa^9$

Table 1 (part 2). Coefficients  $c(n)$  for constants  $\alpha_{\mu\nu}$  of Eq. (42). In this case  $j = 9/2$ .

$n_1$	$n_2$	$n_3$	$n_4$	$c(n)/\rho$
0	0	0	0	$-5120r^4\kappa^6 + 61440r^4\kappa^8$
1	0	0	0	$1024r^3\kappa^5 - 49152r^3\kappa^7 + 122880r^5\kappa^7 + 98304r^3\kappa^9 - 491520r^5\kappa^9$
1	1	0	0	$4480r^2\kappa^6 - 24576r^4\kappa^6 - 71680r^2\kappa^8 + 589824r^4\kappa^8 - 737280r^6\kappa^8$
1	1	1	0	$-53760r^3\kappa^7 + 147456r^5\kappa^7 + 286720r^3\kappa^9 - 1179648r^5\kappa^9 + 983040r^7\kappa^9$
1	1	1	1	$107520r^4\kappa^8 - 196608r^6\kappa^8$
2	0	0	0	$-96r^2\kappa^4 + 128r^2\kappa^6 + 7168r^4\kappa^6 - 45056r^2\kappa^8 - 49152r^4\kappa^8 - 245760r^6\kappa^8$
2	1	0	0	$1856r^3\kappa^5 + 15360r\kappa^7 + 29952r^3\kappa^7 - 55296r^5\kappa^7 - 40960r\kappa^9 + 311296r^3\kappa^9 - 294912r^5\kappa^9 +$ $1474560r^7\kappa^9$
2	1	1	0	$-6656r^4\kappa^6 - 87040r^2\kappa^8 - 141312r^4\kappa^8 - 73728r^6\kappa^8$
2	1	1	1	$-3072r^5\kappa^7 + 51200r^3\kappa^9 + 36864r^5\kappa^9 + 245760r^7\kappa^9$
2	2	0	0	$-48\kappa^4 + 96r^2\kappa^4 - 1536\kappa^6 + 2176r^2\kappa^6 - 16128r^4\kappa^6 - 3328\kappa^8 + 35840r^2\kappa^8 + 59904r^4\kappa^8 +$ $258048r^6\kappa^8$
2	2	1	0	$960r\kappa^5 - 1920r^3\kappa^5 + 18432r\kappa^7 - 50688r^3\kappa^7 + 144384r^5\kappa^7 + 33792r\kappa^9 - 28672r^3\kappa^9 +$ $18432r^5\kappa^9 - 737280r^7\kappa^9$
2	2	1	1	$-3840r^2\kappa^6 + 7680r^4\kappa^6 - 36864r^2\kappa^8 + 150528r^4\kappa^8 - 190464r^6\kappa^8$
2	2	2	0	$768\kappa^6 - 5376r^2\kappa^6 + 10240r^4\kappa^6 + 12288\kappa^8 - 80896r^2\kappa^8 + 43008r^4\kappa^8 - 248832r^6\kappa^8$
2	2	2	1	$-4608r\kappa^7 + 32256r^3\kappa^7 - 61440r^5\kappa^7 - 24576r\kappa^9 + 149504r^3\kappa^9 - 184320r^5\kappa^9 + 399360r^7\kappa^9$
2	2	2	2	$-1536\kappa^8 + 12288r^2\kappa^8 - 33792r^4\kappa^8 + 76800r^6\kappa^8$
3	0	0	0	$-64r^3\kappa^5 + 60672r^3\kappa^7 - 67584r^5\kappa^7 - 57344r^3\kappa^9 + 294912r^5\kappa^9 + 163840r^7\kappa^9$
3	1	0	0	$-8960r^2\kappa^6 + 9728r^4\kappa^6 + 117760r^2\kappa^8 - 964608r^4\kappa^8 + 712704r^6\kappa^8$
3	1	1	0	$107520r^3\kappa^7 - 107520r^5\kappa^7 - 542720r^3\kappa^9 + 2330624r^5\kappa^9 - 1228800r^7\kappa^9$
3	1	1	1	$-215040r^4\kappa^8 + 208896r^6\kappa^8$
3	2	0	0	$960r\kappa^5 - 896r^3\kappa^5 + 3072r\kappa^7 - 70656r^3\kappa^7 + 98304r^5\kappa^7 + 64512r\kappa^9 - 231424r^3\kappa^9 +$ $374784r^5\kappa^9 - 983040r^7\kappa^9$
3	2	1	0	$-15360r^2\kappa^6 + 14336r^4\kappa^6 - 96256r^2\kappa^8 + 546816r^4\kappa^8 - 524288r^6\kappa^8$
3	2	1	1	$46080r^3\kappa^7 - 43008r^5\kappa^7 + 167936r^3\kappa^9 - 528384r^5\kappa^9 + 262144r^7\kappa^9$
3	2	2	0	$-13824r\kappa^7 + 105984r^3\kappa^7 - 104448r^5\kappa^7 - 94208r\kappa^9 + 296960r^3\kappa^9 - 446464r^5\kappa^9 +$ $878592r^7\kappa^9$
3	2	2	1	$55296r^2\kappa^8 - 423936r^4\kappa^8 + 417792r^6\kappa^8$
3	2	2	2	$12288r\kappa^9 - 73728r^3\kappa^9 + 282624r^5\kappa^9 - 352256r^7\kappa^9$
3	3	0	0	$640r^2\kappa^6 - 512r^4\kappa^6 - 82944r^2\kappa^8 + 337920r^4\kappa^8 - 202752r^6\kappa^8$
3	3	1	0	$-7680r^3\kappa^7 + 6144r^5\kappa^7 + 475136r^3\kappa^9 - 1404928r^5\kappa^9 + 679936r^7\kappa^9$
3	3	1	1	$15360r^4\kappa^8 - 12288r^6\kappa^8$
3	3	2	0	$91136r^2\kappa^8 - 353280r^4\kappa^8 + 229376r^6\kappa^8$
3	3	2	1	$-182272r^3\kappa^9 + 706560r^5\kappa^9 - 458752r^7\kappa^9$
3	3	3	0	$-108544r^3\kappa^9 + 260096r^5\kappa^9 - 114688r^7\kappa^9$

Table 2 (part 1). Coefficients  $c(n)$  for constants  $\beta_{\mu\nu}$  of Eq. (42). In this case  $j = 9/2$ .



$n_1$	$n_2$	$n_3$	$n_4$	$c(n)/\rho$
4	0	0	0	$-2432r^2\kappa^6 + 1792r^4\kappa^6 + 37888r^2\kappa^8 - 167424r^4\kappa^8 + 151552r^6\kappa^8$
4	1	0	0	$-15360r\kappa^7 + 85248r^3\kappa^7 - 56832r^5\kappa^7 + 51200r\kappa^9 - 456704r^3\kappa^9 + 1276928r^5\kappa^9 -$ $860160r^7\kappa^9$
4	1	1	0	$122880r^2\kappa^8 - 506880r^4\kappa^8 + 325632r^6\kappa^8$
4	1	1	1	$-122880r^3\kappa^9 + 448512r^5\kappa^9 - 282624r^7\kappa^9$
4	2	0	0	$768\kappa^6 - 2176r^2\kappa^6 + 2048r^4\kappa^6 - 5632\kappa^8 + 1536r^2\kappa^8 + 61440r^4\kappa^8 - 134656r^6\kappa^8$
4	2	1	0	$-9216r\kappa^7 + 26112r^3\kappa^7 - 24576r^5\kappa^7 + 2048r\kappa^9 - 22528r^3\kappa^9 - 110592r^5\kappa^9 + 309248r^7\kappa^9$
4	2	1	1	$18432r^2\kappa^8 - 52224r^4\kappa^8 + 49152r^6\kappa^8$
4	2	2	0	$-7680\kappa^8 + 71680r^2\kappa^8 - 175104r^4\kappa^8 + 156672r^6\kappa^8$
4	2	2	1	$15360r\kappa^9 - 143360r^3\kappa^9 + 350208r^5\kappa^9 - 313344r^7\kappa^9$
4	3	0	0	$10752r\kappa^7 - 28416r^3\kappa^7 + 12288r^5\kappa^7 - 50176r\kappa^9 + 347136r^3\kappa^9 - 727040r^5\kappa^9 + 404480r^7\kappa^9$
4	3	1	0	$-86016r^2\kappa^8 + 227328r^4\kappa^8 - 98304r^6\kappa^8$
4	3	1	1	$86016r^3\kappa^9 - 227328r^5\kappa^9 + 98304r^7\kappa^9$
4	3	2	0	$51200r\kappa^9 - 245760r^3\kappa^9 + 495616r^5\kappa^9 - 331776r^7\kappa^9$
4	4	0	0	$7424\kappa^8 - 44032r^2\kappa^8 + 62976r^4\kappa^8 - 21504r^6\kappa^8$
4	4	1	0	$-29696r\kappa^9 + 176128r^3\kappa^9 - 251904r^5\kappa^9 + 86016r^7\kappa^9$
5	0	0	0	$2304r^3\kappa^7 - 1536r^5\kappa^7 - 20480r^3\kappa^9 + 91136r^5\kappa^9 - 106496r^7\kappa^9$
5	1	0	0	$25600r^2\kappa^8 - 86016r^4\kappa^8 + 51200r^6\kappa^8$
5	1	1	0	$-102400r^3\kappa^9 + 288768r^5\kappa^9 - 167936r^7\kappa^9$
5	2	0	0	$-4608r\kappa^7 + 9984r^3\kappa^7 - 6144r^5\kappa^7 + 1024r\kappa^9 - 11264r^3\kappa^9 - 22528r^5\kappa^9 + 113664r^7\kappa^9$
5	2	1	0	$36864r^2\kappa^8 - 79872r^4\kappa^8 + 49152r^6\kappa^8$
5	2	1	1	$-36864r^3\kappa^9 + 79872r^5\kappa^9 - 49152r^7\kappa^9$
5	2	2	0	$15360r\kappa^9 - 81920r^3\kappa^9 + 141312r^5\kappa^9 - 116736r^7\kappa^9$
5	3	0	0	$-7168r^2\kappa^8 + 18432r^4\kappa^8 - 8192r^6\kappa^8$
5	3	1	0	$28672r^3\kappa^9 - 73728r^5\kappa^9 + 32768r^7\kappa^9$
5	4	0	0	$-19456r\kappa^9 + 67584r^3\kappa^9 - 71680r^5\kappa^9 + 20480r^7\kappa^9$
6	0	0	0	$-6656r^2\kappa^8 + 12288r^4\kappa^8 - 5632r^6\kappa^8$
6	1	0	0	$-10240r\kappa^9 + 44032r^3\kappa^9 - 51200r^5\kappa^9 + 17408r^7\kappa^9$
6	2	0	0	$-1536\kappa^8 + 17408r^2\kappa^8 - 29184r^4\kappa^8 + 13312r^6\kappa^8$
6	2	1	0	$6144r\kappa^9 - 69632r^3\kappa^9 + 116736r^5\kappa^9 - 53248r^7\kappa^9$
6	3	0	0	$13312r\kappa^9 - 38912r^3\kappa^9 + 35840r^5\kappa^9 - 10240r^7\kappa^9$
7	0	0	0	$7168r^3\kappa^9 - 14336r^5\kappa^9 + 7168r^7\kappa^9$
7	2	0	0	$3072r\kappa^9 - 16384r^3\kappa^9 + 23552r^5\kappa^9 - 10240r^7\kappa^9$

Table 2 (part 2). Coefficients  $c(n)$  for constants  $\beta_{\mu\nu}$  of Eq. (42). In this case  $j = 9/2$ .

## C Sample Constant Field and Sample Points

The constant field  $a_\mu$  used in numerical calculations of Sec. 4.1 (see Eq. (56)) is specified by

$$a_0 = \begin{pmatrix} 0.333027 & 0.438189 + 0.318128i & 0.374405 + 0.222978i \\ 0.438189 - 0.318128i & -0.154498 & 0.378804 + 0.22751i \\ 0.374405 - 0.222978i & 0.378804 - 0.22751i & -0.178529 \end{pmatrix}$$

$$a_1 = \begin{pmatrix} 0.230383 & 0.202411 + 0.030092i & 0.384110 - 0.364239i \\ 0.202411 - 0.030092i & -0.162558 & 0.448044 - 0.138645i \\ 0.384110 + 0.364239i & 0.448044 + 0.138645i & -0.067824 \end{pmatrix}$$

$$a_2 = \begin{pmatrix} -0.254314 & 0.490871 - 0.296415i & 0.709724 - 0.352729i \\ 0.490871 + 0.296415i & 0.330503 & 0.970160 + 0.109804i \\ 0.709724 + 0.352729i & 0.970160 - 0.109804i & -0.076189 \end{pmatrix}$$

$$a_3 = \begin{pmatrix} -0.055155 & 0.502826 + 0.023544i & 0.435721 - 0.074859i \\ 0.502826 - 0.023544i & 0.159857 & 0.581485 + 0.032500i \\ 0.435721 + 0.074859i & 0.581485 - 0.032500i & -0.104703 \end{pmatrix}$$

The classical limit on non-constant backgrounds was evaluated at the following randomly generated points on the unit symmetric torus.

x	y	z	t
0.103172983143503	0.9458719000957324	0.956116383180309	0.438505993255755
0.248194925172178	0.0893431271786154	0.336764036419274	0.118409829321844
0.174820791004537	0.7529966955146729	0.984186866641149	0.265965702089591
0.450532157114747	0.7958101168552333	0.274186255621803	0.321281009101127
0.416208702090845	0.6286435317521117	0.459165616384016	0.356014499573743
0.295893446617454	0.0590763301619042	0.678511201131179	0.781239724758651
0.192720463473952	0.1132044300661718	0.722394817950870	0.342733731502896
0.944525538301774	0.0238613028875564	0.385630781531596	0.224323902181052
0.769704747297237	0.2708646073728835	0.401443914890447	0.958358200091461
0.319172590182490	0.4750544905176503	0.127257659268644	0.637077190990334

## References

- [1] I. Horváth, [hep-lat/0607031](#).
- [2] I. Horváth, PoS **LAT2006** (2006) 053, [hep-lat/0610121](#).
- [3] I. Horváth, Phys. Rev. Lett. **81** (1998) 4063; I. Horváth, Phys. Rev. **D60** (1999) 034510; I. Horváth, C.T. Balwe, R. Mendris, Nucl. Phys. **B599**, 283 (2001).
- [4] H. Neuberger, Phys. Lett. **B417** (1998) 141; Phys. Lett. **B427** (1998) 353.
- [5] P. Hernández, K. Jansen, M. Lüscher, Nucl. Phys. **B552**, 363 (1999).
- [6] T. Draper *et al*, [hep-lat/0609034](#).
- [7] I. Horváth, A. Alexandru, J.B. Zhang, Y. Chen, S.J. Dong, T. Draper, K.F. Liu, N. Mathur, S. Tamhankar, H.B. Thacker, Phys. Lett. **B617** (2005) 49.
- [8] P. Hasenfratz, V. Laliena, F. Niedermayer, Phys. Lett. **B427** (1998) 125.
- [9] R. Narayanan and H. Neuberger, Nucl. Phys. **B443**, 305 (1995).
- [10] Y. Kikukawa and A. Yamada, Phys. Lett. **B448** (1999) 265.
- [11] K. Fujikawa, Nucl. Phys. **B546** (1999) 480; D. Adams, Annals Phys. **296** (2002) 131; H. Suzuki, Prog. Theor. Phys. **102** (1999) 141; D. Adams, J. Math. Phys. **42** (2001) 5522.
- [12] I. Horváth *et al.*, [hep-lat/0212013](#). Proceedings of the "Quark Confinement and the Hadron Spectrum V", Gargnano, Italy, Sep 10-14, 2002, N. Brambilla and G. Proserpi editors, World Scientific (2003) p.312.
- [13] I. Horváth, S.J. Dong, T. Draper, F.X. Lee, K.F. Liu, N. Mathur, H.B. Thacker, J.B. Zhang, Phys. Rev. **D68**, 114505 (2003).
- [14] Y. Chen *et al.*, Phys. Rev. **D73** 014516 (2006).
- [15] F. Niedermayer, Nucl. Phys. **B** (Proc. Suppl.) 73, 105 (1999).
- [16] K.F. Liu, PoS **LAT2006** (2006) 056, [hep-lat/0609033](#).
- [17] K.F. Liu, A. Alexandru, I. Horváth, Phys. Lett. **B659** (2008) 773, [hep-lat/0703010](#).
- [18] M. Constantinou, H. Panagopoulos, Phys. Rev. **D76** (2007) 114504.
- [19] C. Alexandrou, H. Panagopoulos, E. Vicari, Nucl. Phys. **B571** (2000) 257.
- [20] D. Adams, private communication.
- [21] I. Horváth, A. Alexandru, J.B. Zhang, S.J. Dong, T. Draper, F.X. Lee, K.F. Liu, N. Mathur, H.B. Thacker, Phys. Lett. **B612** (2005) 21.

- [22] A. Alexandru, I. Horváth, J.B. Zhang, Phys. Rev. **D72** (2005) 034506.
- [23] S. Ahmad, J.T. Lenaghan, H.B. Thacker, Phys. Rev. **D72**, 114511 (2005).
- [24] E.M. Ilgenfritz, K. Koller, Y. Koma, G. Schierholz, T. Streuer, V. Weinberg, Phys. Rev. **D76**, 034506 (2007).
- [25] N. Mathur, F.X. Lee, A. Alexandru, C. Bennhold, Y. Chen, S.J. Dong, T. Draper, I. Horváth, K.F. Liu, S. Tamhankar, J.B. Zhang, Phys. Rev. **D70** (2004) 074508.
- [26] N. Mathur, A. Alexandru, Y. Chen, S.J. Dong, T. Draper, I. Horváth, F.X. Lee, K.F. Liu, S. Tamhankar, J.B. Zhang, Phys. Rev. **D76** (2007) 114505.